

Supporting Information

Rapid Photoswitching of Low Molecular Weight Arylazoisoxazole Adhesives

Luuk Kortekaas,^{1,*} Julian Simke,¹ Dustin W. Kurka¹ and Bart Jan Ravoo^{1,*}

¹Center for Soft Nanoscience and Organisch-Chemisches Institut, Westfälische Wilhelms-Universität Münster, Busso-Peus-Straße 10, 48149 Münster, Germany

Corresponding authors

Luuk Kortekaas - Center for Soft Nanoscience and Organisch-Chemisches Institut, Westfälische Wilhelms-Universität Münster, Busso-Peus-Straße 10, 48149 Münster, Germany; ORCID orcid.org/0000-0002-3420-4349; Phone: +49 251 83 34514; Email: kortekaas@wwu.de

Bart Jan Ravoo - Center for Soft Nanoscience and Organisch-Chemisches Institut, Westfälische Wilhelms-Universität Münster, Busso-Peus-Straße 10, 48149 Münster, Germany; Phone: +49 251 83 33287; Email: b.j.ravoo@uni-muenster.de; Fax: +49 251 83 36557

Table of Contents

Supporting Graphics.....	S2
Figure S1 Photofatigue resistance of AIZs 1, 3 and 4.....	S2
Figure S2 Photoisomerization by ¹ H NMR spectroscopy.....	S2
Table S1 Photostationary states and half-lives.....	S4
Figure S3 Thermal reversion by UV/vis spectroscopy.....	S5
Figure S4 Differential Scanning Calorimetry.....	S5
Figure S5 Thin film absorption and ¹ H NMR spectroscopy after liquefaction.....	S6
Figure S6 Photographs of the different steps in the cohesion methodology.....	S6
Figure S7 Picture of formerly cohered slides after UV-induced adhesive failure.....	S7
Figure S8 Underwater cohesive durability.....	S7
Figure S9 Maximum weight bearing at glass slides cohered with AIZ 2.....	S8
Figure S10 Tensometry of AIZ 2.....	S8
Figure S11 Microscopy of the adhesive layer of AIZ 2.....	S8
Figure S12 Maximum weight bearing at conjoined plexiglass/glass with AIZ 2.....	S9
Figure S13 Maximum weight bearing at plexiglass slides cohered with AIZ 2.....	S9
Experimental Procedures.....	S10
Materials.....	S10
Syntheses.....	S10
Precursors 9-11.....	S10
Compounds 5-8.....	S14
AIZs 1-4.....	S18
Characterization Methods.....	S23
Crystal structure analysis of AIZs 1-4.....	S25
Supporting References.....	S29

SUPPORTING GRAPHICS

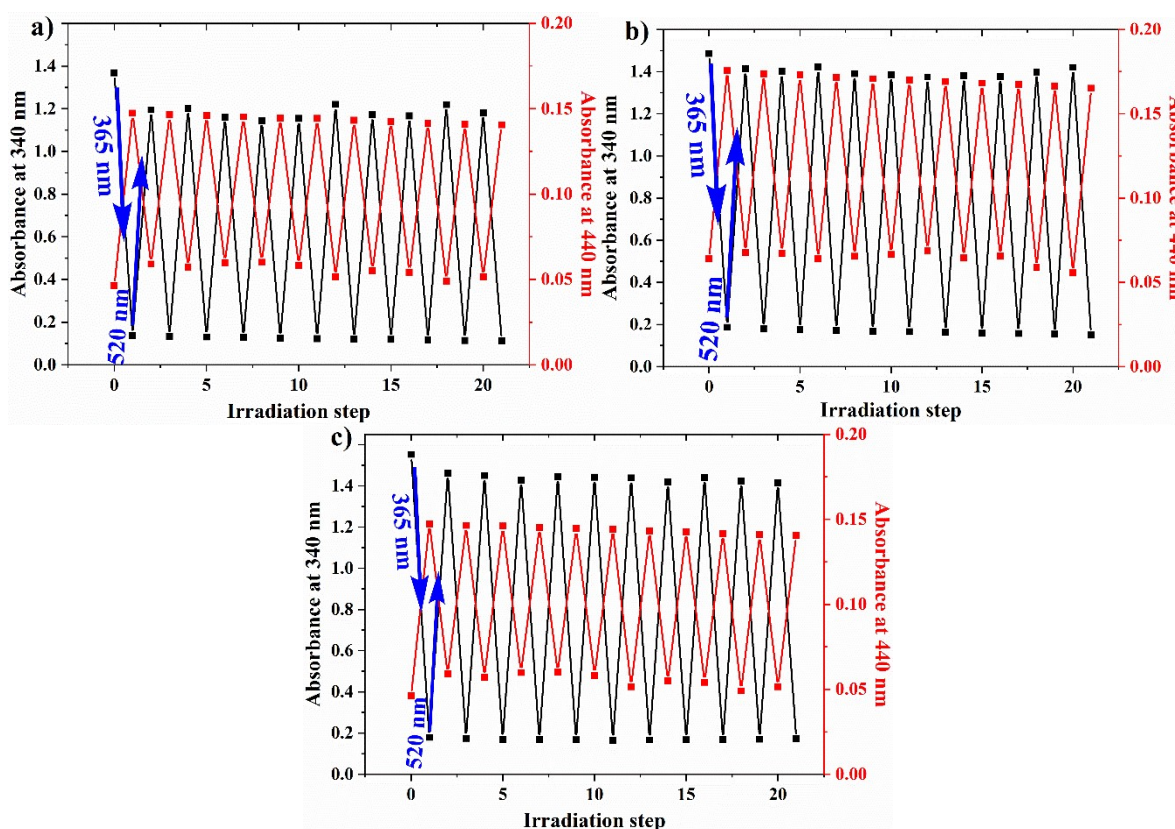
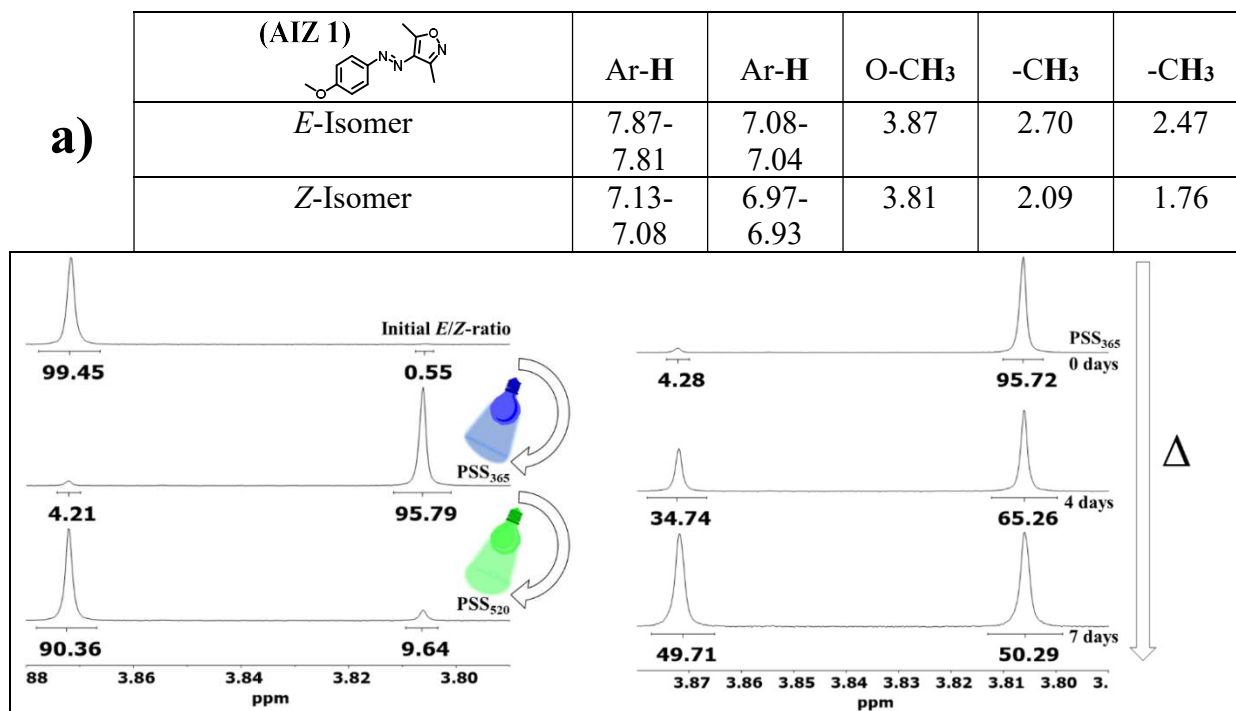


Figure S1 | Photofatigue resistance of AIZs 1, 3 and 4. Evolution in absorbance of a 70 μ M solution of (a) 1, (b) 3 and (c) 4 in acetonitrile at 340 nm (black vertical axis) and 440 nm (red vertical axis) after alternating irradiation steps for 3 s at 365 nm (radiant flux 1.2 W, $E \rightarrow Z$ -isomerization) and 40 s at 520 nm (87 lm, $Z \rightarrow E$ -isomerization).

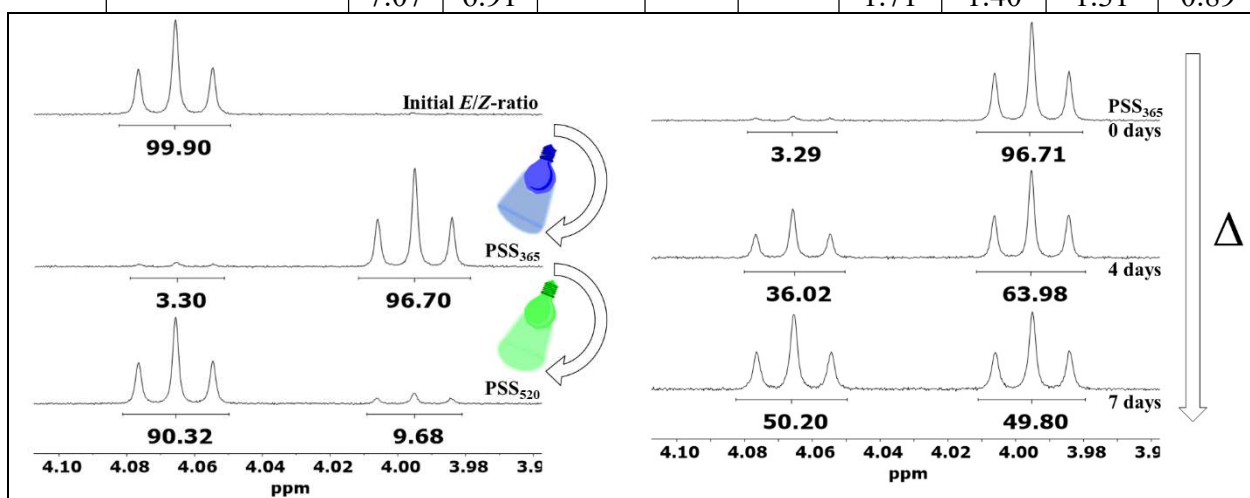


b)

(AIZ 2)	Ar-H	Ar-H	O-CH ₂	-CH ₃	-CH ₃	-CH ₂ -	-(CH ₂) ₂ -CH ₃	-CH ₂ -CH ₃
<i>E</i> -Isomer	7.96-7.72	7.15-6.95	4.07	2.70	2.47	1.81-1.76	1.48-1.37	0.94
<i>Z</i> -Isomer	7.11-7.04	6.95-6.89	4.00	2.09	1.75	1.77-1.73	1.45-1.35	0.92

c)

(AIZ 3)	Ar-H	Ar-H	O-CH ₂	-CH ₃	-CH ₃	-CH ₂ -	-CH ₂ -	-(CH ₂) ₂ -CH ₃	-CH ₂ -CH ₃
<i>E</i> -Isomer	7.83-7.79	7.06-7.02	4.07	2.70	2.47	1.81-1.75	1.50-1.44	1.39-1.33	0.93-0.90
<i>Z</i> -Isomer	7.10-7.07	6.94-6.91	4.00	2.09	1.75	1.77-1.71	1.48-1.40	1.37-1.31	0.92-0.89



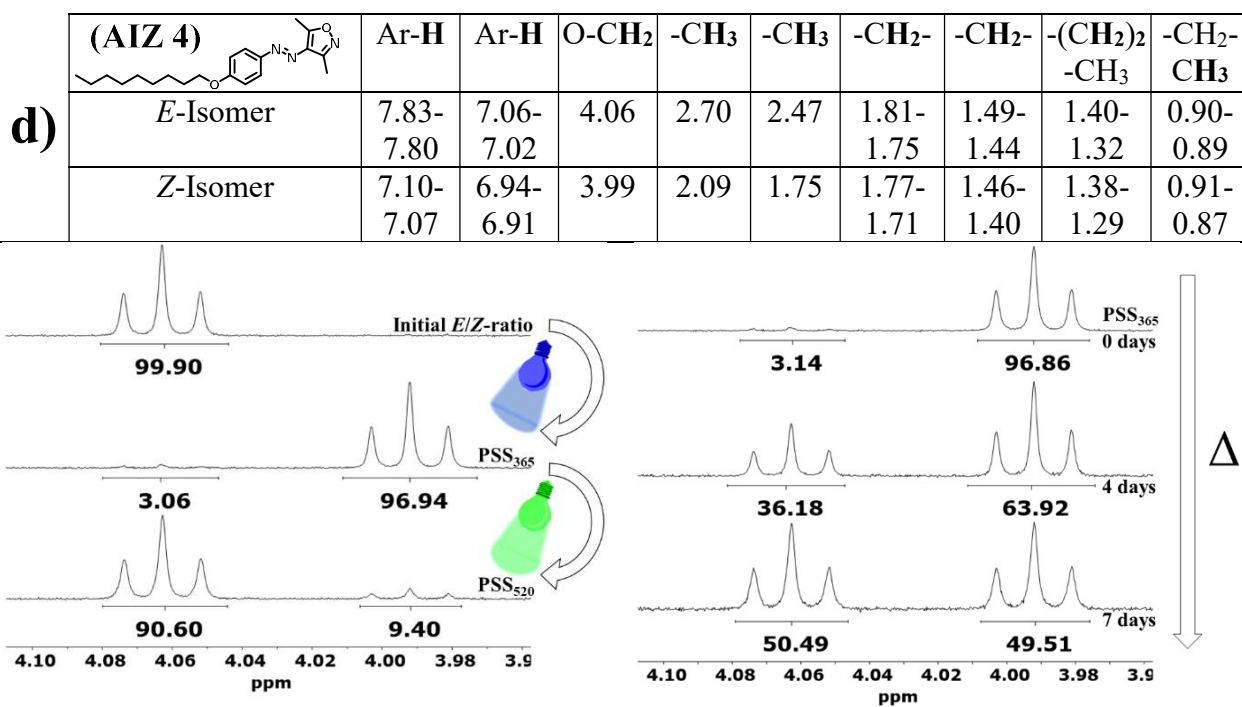


Figure S2 | Photoisomerization by ¹H NMR spectroscopy. ¹H NMR chemical shifts of the *Z*- and *E*-form of AIZs (a) **1**, (b) **2**, (c) **3** and (d) **4** in acetonitrile-*d*₃ with the change in chemical shifts shown of the first methyl unit off the phenol moiety to demonstrate the PSSs and thermal relaxation after UV-induced *E*→*Z*-isomerization (for the NMR spectra of compound **2**, see Figure 1 in main text).

Table S1 | Photostationary states and half-lives. The thermal isomer distribution, PSSs and half-lives of compounds **1-4** as determined by ¹H NMR spectroscopy.

Compound	Initial <i>E/Z</i> -ratio	PSS ₃₆₅	PSS ₅₂₀	<i>t</i> _{1/2} PSS ₃₆₅ → <i>E</i>
1	99:1	96%	90%	7 d
2	>99	97%	91%	7 d
3	>99	97%	90%	7 d
4	>99	97%	91%	7 d

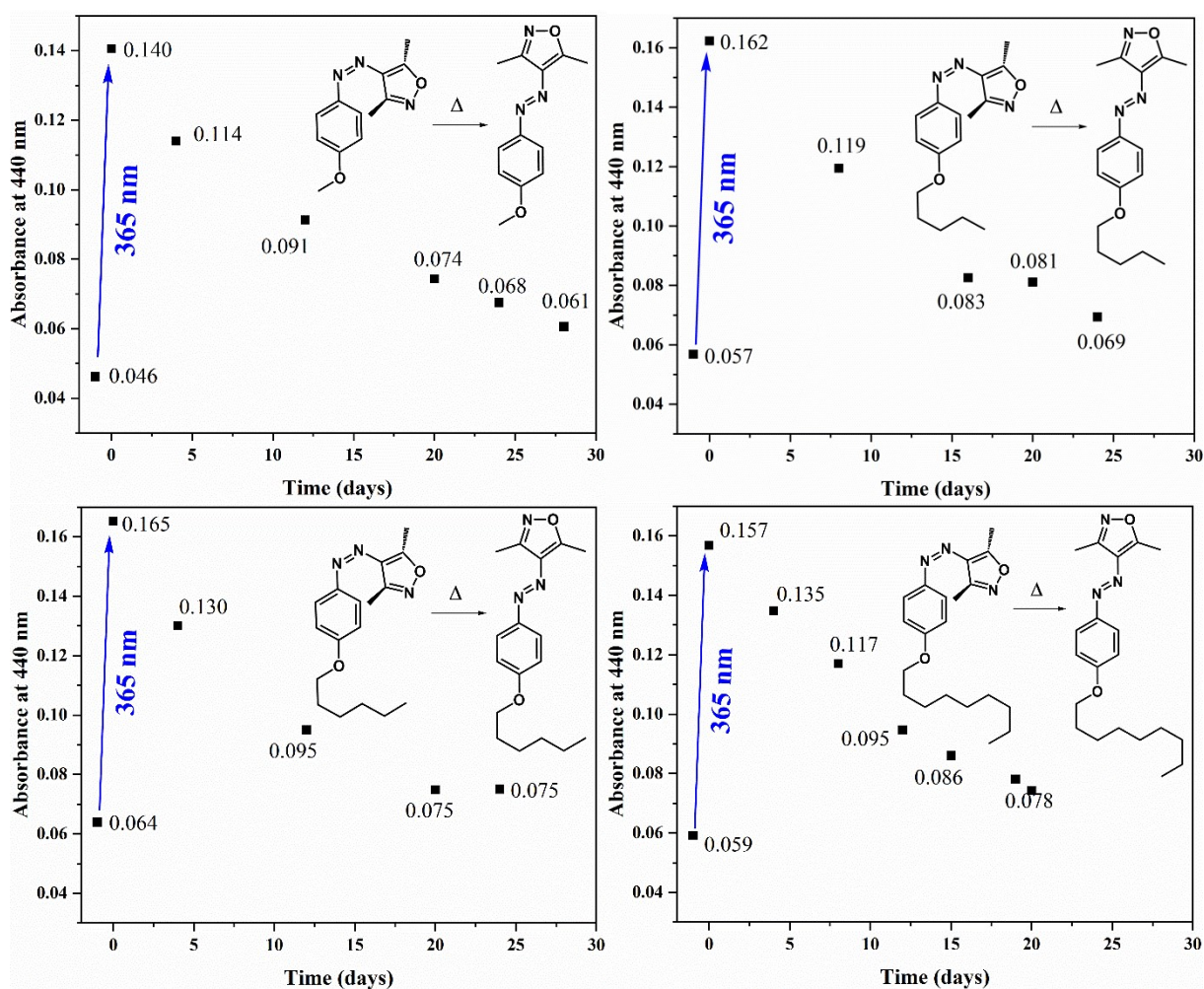


Figure S3 | Thermal reversion by UV/vis spectroscopy. Evolution of the absorbance of compounds 1, 2, 3 and 4 over time after reaching the PSS₃₆₅.

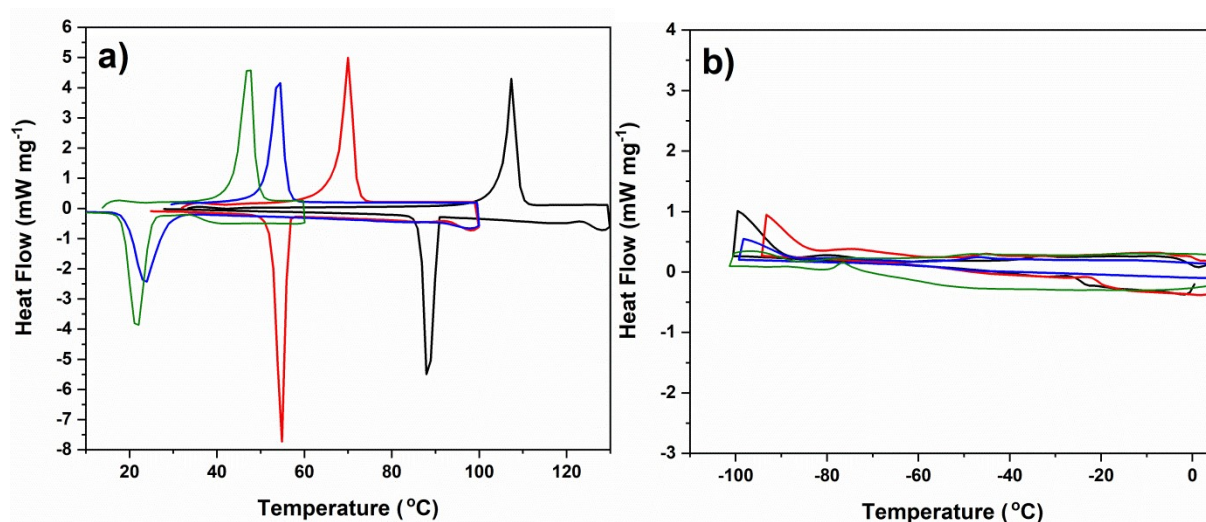


Figure S4 | Differential Scanning Calorimetry. DSC thermograms of azoisoxazoles 1 (black), 2 (red), 3 (blue) and 4 (green) before (a) and after (b) light-induced solid-to-liquid phase transition at 365 nm (heating rate of 10 °C min⁻¹).

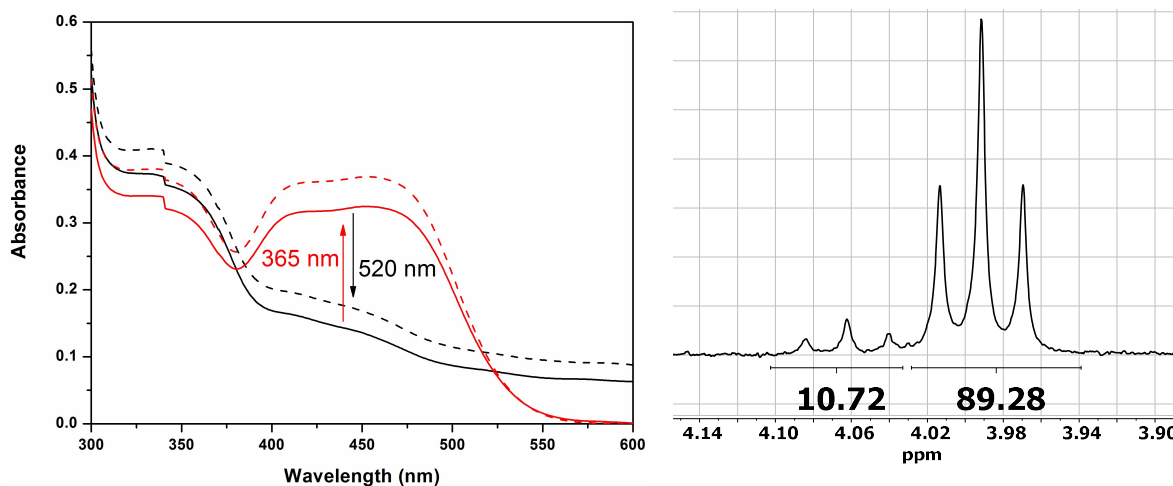


Figure S5. | Thin film absorption and ^1H NMR spectroscopy after liquefaction. (Left) Absorption spectra of a thin film of **2** pressed between 2 glass slides before (black solid) and after (red solid) irradiation at 365 nm with concurrent solid-to-liquid phase-transitioning. Subsequent irradiation at 520 nm resolidifies the AIZ with simultaneous loss of visible absorption (black dashed), and this process can be repeated (dashed lines). The rise in baseline in the solid state thin film (*E*-form) is due to scattering of incident light. (Right) ^1H NMR spectroscopy of AIZ **2** after solid state switching. The photoliquefaction of AIZ was performed on a glass slide, analogous to the procedure for glass cohesion, and the resulting liquid was fully dissolved in acetonitrile- d_3 in the dark. The marker bands were thus used to determine a composition of 89% *Z*- and 11% *E*-form at the PSS_{365} in the solid state.



Figure S6 | Photographs of the different steps in the cohesion methodology. The applied methodology for conjoining glass slides with AIZ adhesives. (Left) Weighing out 2.1 mg of arylazo-3,5-dimethylisoxazole within a 1.4 x 1.0 cm surface of a glass slide. (Middle) Irradiation at 365 nm to cause a solid-to-liquid phase transition. (Right) pressing two 1.4 x 1.0 cm overlapping glass surfaces together and irradiating at 520 nm to induce the liquid-to-solid phase transition.



Figure S7 | Photograph of formerly cohered slides after UV-induced adhesive failure. The glass slides after photochemically induced separation of compound **1** from the interface at the right-hand glass slide.

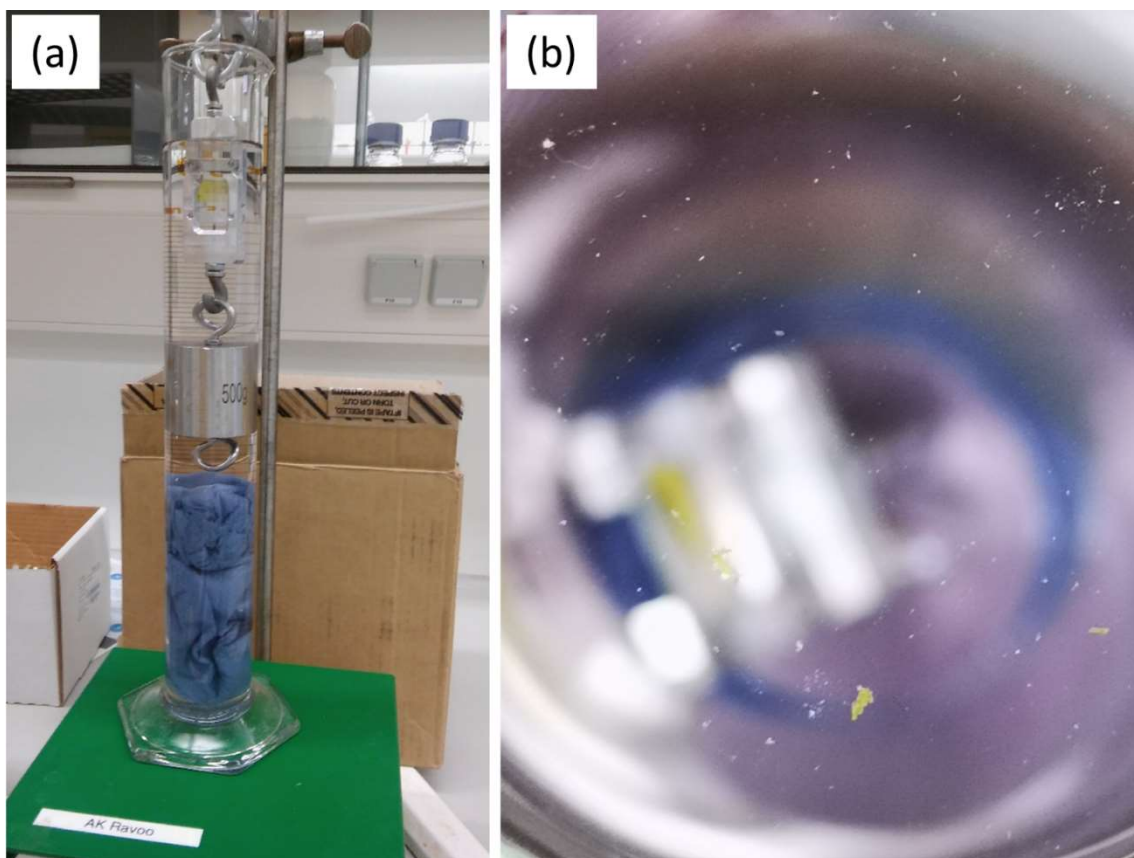


Figure S8 | Underwater cohesive durability. (a) Testing the water-resistance of compound **3** as an adhesive. The composite succumbed to the 500 g weight after immersion in water for 21 minutes. (b) Physical rupture causes part of the compound to detach from the surface, hindering its full reversibility.



Figure S9 | Maximum weight bearing at glass slides cohered with AIZ 2. Suspension of glass slides conjoined with 2.1 mg of compound **2** at a 1.0 by 1.4 cm overlapping surface area, bearing a load of 4.4 kg without breaking.

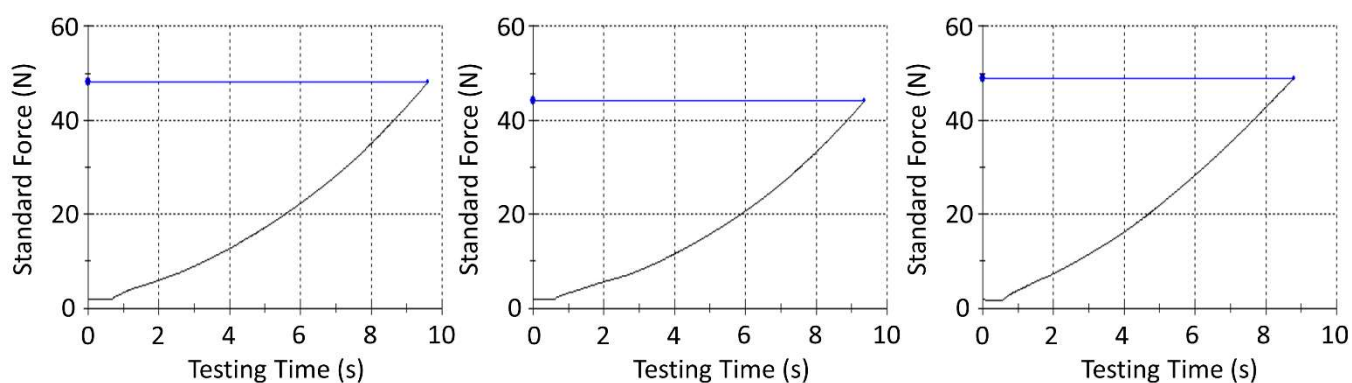


Figure S10 | Tensometry of AIZ 2. Tensile strength measurements of 3 pairs of glass slides conjoined at a 1.0 by 1.4 cm area with 2.1 mg of **2** as shown in Scheme 2b, showing break points at a standard force of 48.15 N, 44.09 N and 48.97 N (i.e., 47.1 ± 2.1 N).

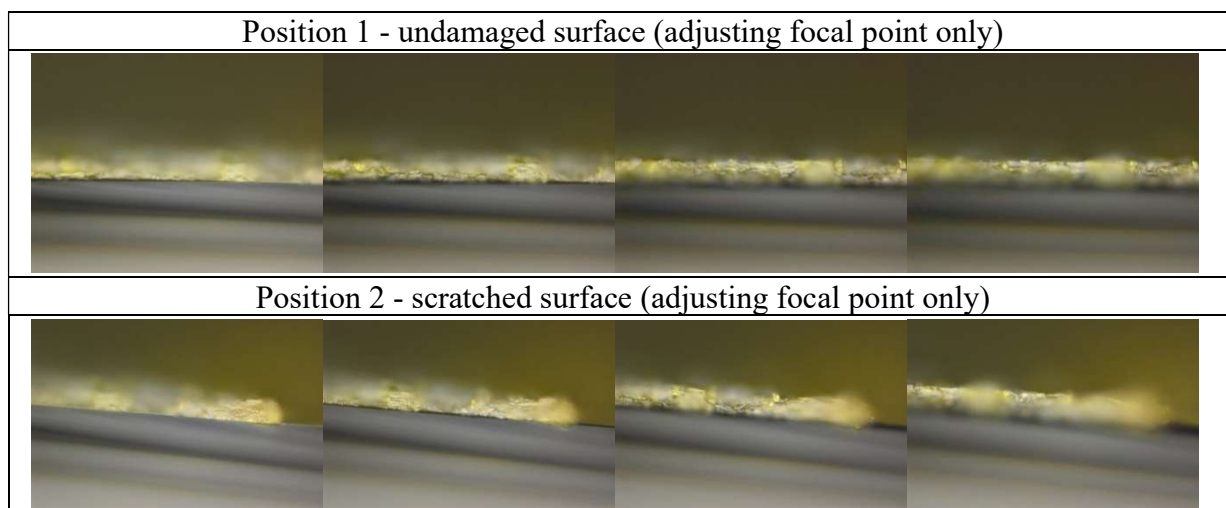


Figure S11 | Microscopy of the adhesive layer of AIZ 2. Microscopy images of the layer of compound **2** after photoreversed adhesion of glass slides. The slides were photochemically conjoined as usual (Scheme 2b) with 2.1 mg of compound **2**, and suspended with 2 kg before irradiating at 365 nm. Immediately after rupture the slide was irradiated at 520 nm to harden the still adhesive layer on the slide that did not undergo the adhesive failure. (Top) Different focus of the same representative layer of compound **2**. (Bottom) The adhesive layer after perpendicular scratching with a needle.



Figure S12 | Maximum weight bearing at conjoined plexiglass (PMMA) and glass with AIZ 2. Suspension of glass slides conjoined with 2.1 mg of compound **2** at a 1.0 by 1.4 cm overlapping surface area, bearing a load of 3.8 kg without rupture.

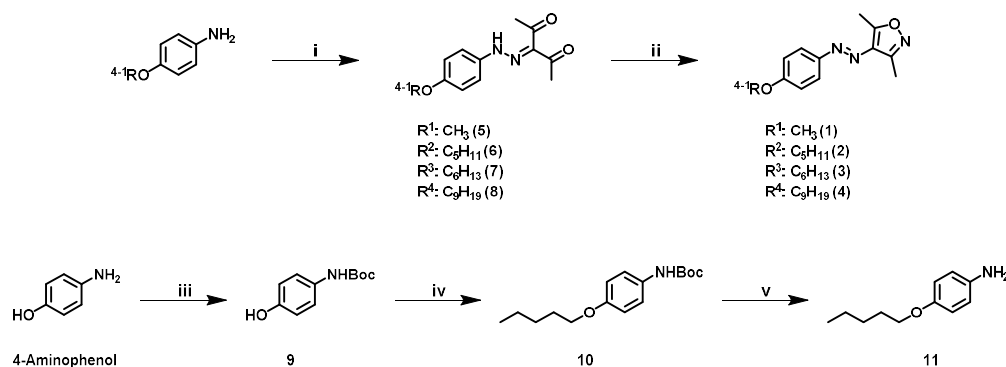


Figure S13 | Maximum weight bearing at plexiglass (PMMA) slides cohered with AIZ 2. Suspension of plexiglass (PMMA) slides conjoined with 2.2 mg of compound **2** at a 1.0 by 1.4 cm overlapping surface area, capable of bearing a load of up to 3.5 kg without rupture.

EXPERIMENTAL PROCEDURES

Syntheses

The syntheses of AIZs **1-4** were carried out through general procedures I and II, starting from 4-(methoxy)-, 4-(*n*-pentyloxy)-, 4-(*n*-hexyloxy)- and 4-(*n*-nonyloxy)aniline, respectively (Scheme S1). While the aniline starting materials for target compounds **1**, **3** and **4** are commercially available, 4-(*n*-pentyloxy)aniline was prepared in a three-step synthesis as described firstly below. In general, diazotization of the aniline starting materials and subsequent azo coupling with pentane-2,4-dione provides the substituted 3-(2-phenylhydrazono)pentane-2,4-diones, with a subsequent cyclization step using hydroxylamine hydrochloride yielding AIZs **1-4**.



Scheme S1. General overview of the syntheses of the substituted AIZ target compounds. Reaction conditions: i) AcOH, HCl, NaNO₂, NaOAc, pentane-2,4-dione; ii) hydroxylamine hydrochloride, Na₂CO₃; iii) Boc anhydride; iv) 1-bromopentane, K₂CO₃; v) TFA.

Synthetic Procedure for Precursors 9-11 for AIZ 2

Synthesis of *tert*-butyl (4-hydroxyphenyl)carbamate (9**)**^[S3] 4-Aminophenol (1.14 g, 10.5 mmol, 1.0 eq.) was suspended in THF (10 mL) and Boc₂O (2.33 g, 10.7 mmol, 1.02 eq.) was added. The mixture was stirred for 18 h at rt. THF was removed and EtOAc (30 mL) was added. Washing with H₂O (2× 30 mL), drying over MgSO₄ and removing solvent under reduced pressure yielded **9** as a colorless solid (2.04 g, 9.75 mmol, 93%).

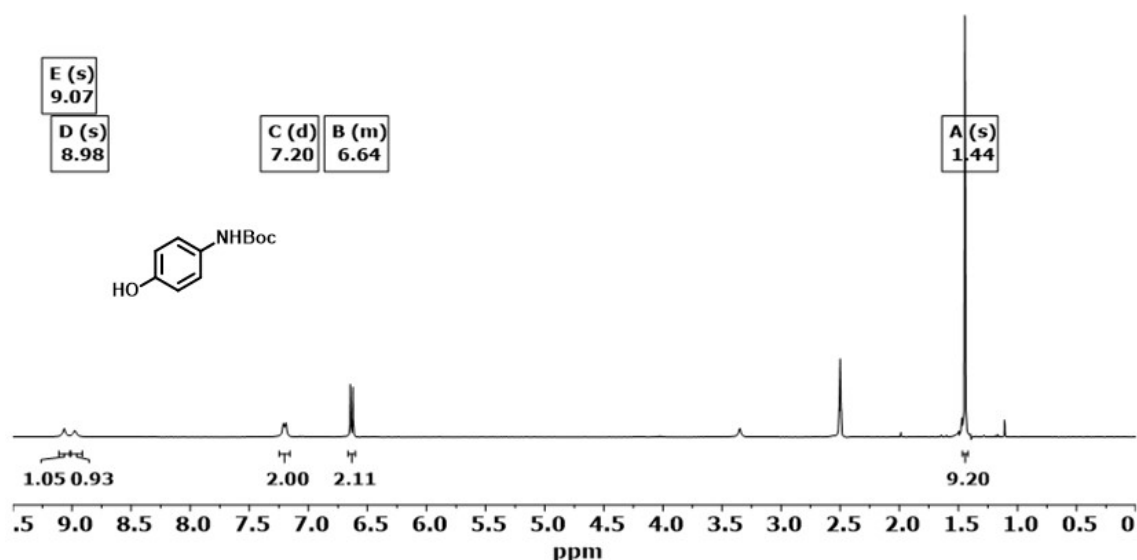


Figure S14. ^1H -NMR spectrum of **9** (DMSO- d_6 , 400 MHz): δ = 9.07 (s, 1H, -N-H), 8.98 (s, 1H, -O-H), 7.20 (d, J = 8.4 Hz, 2H, Ar-H) 6.66-6.58 (m, 2H, Ar-H), 1.44 (s, 9H, Boc) ppm.

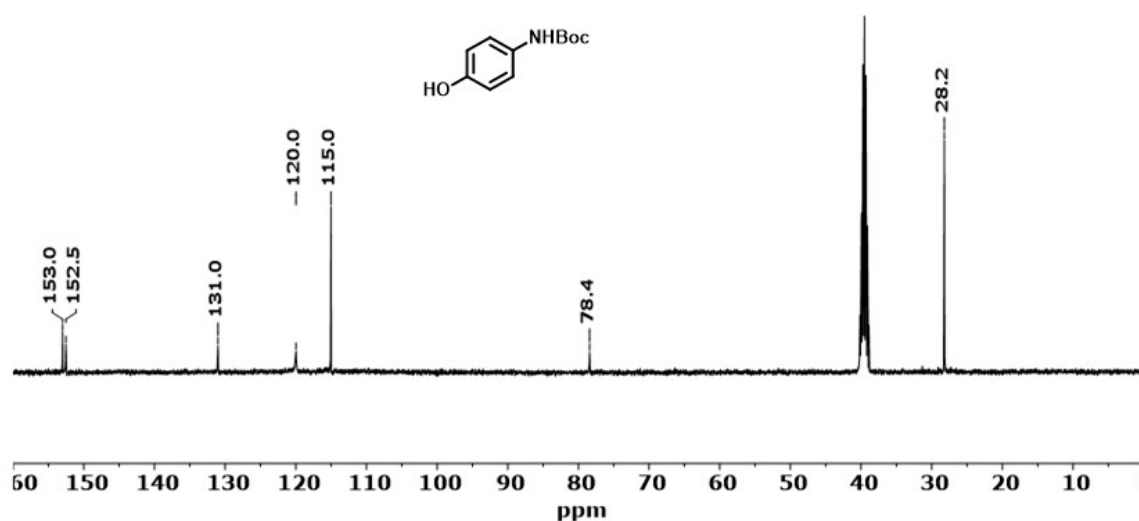


Figure S15. ^{13}C -NMR spectrum of **9** (DMSO- d_6 , 101 MHz): δ = 153.0 (-HN-C-O $_2$ -), 152.5 (Ar-C-OH), 131.0 (Ar-C-NHBoc), 120.0 (Ar-C), 115.0 (Ar-C), 78.4 (-C-(CH $_3$) $_3$), 28.2 (-C-(CH $_3$) $_3$) ppm.

MS (m/z): (ESI, MeOH) Calculated for $[\text{C}_{11}\text{H}_{15}\text{NO}_3\text{Na}]^+$: 232.0944; found 232.0942.

Synthesis of *tert*-butyl (4-(*n*-pentyloxy)phenyl)carbamate (**10**)

9 (1.02 g, 4.88 mmol, 1.0 eq.) was dissolved in ACN (60 mL) and 1-Bromopentane (1.21 mL, 9.76 mmol, 2.0 eq.) and K_2CO_3 (3.37 g, 24.4 mmol, 5.0 eq) were added subsequently. The mixture was stirred for 18 h at 90 °C. After K_2CO_3 was filtered off, the solvent was removed in vacuo and the raw product was purified *via* column chromatography

(silica, CH/EtOAc 9:1). The desired compound **10** was yielded as a colorless solid (1.20 g, 4.30 mmol, 88%).

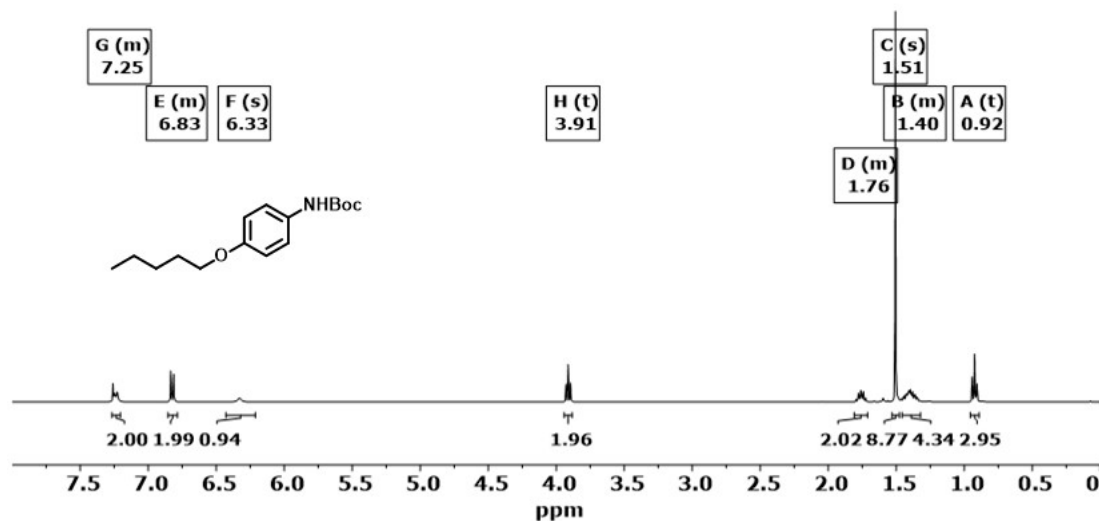


Figure S16. ^1H -NMR spectrum of **10** (Chloroform-*d*, 400 MHz): δ = 7.29-7.15 (m, 2H, Ar-**H**), 6.89-6.73 (m, 2H, Ar-**H**), 6.33 (s, 1H, -N-**H**), 3.91 (t, J = 6.6 Hz, 2H, O-**CH**₂-), 1.81-1.69 (m, 2H, -**CH**₂-), 1.51 (s, 9H, **Boc**) 1.46-1.28 (m, 4H, -(**CH**₂)₂-), 0.92 (t, J = 7.1 Hz, 3H, -**CH**₂-**CH**₃) ppm.

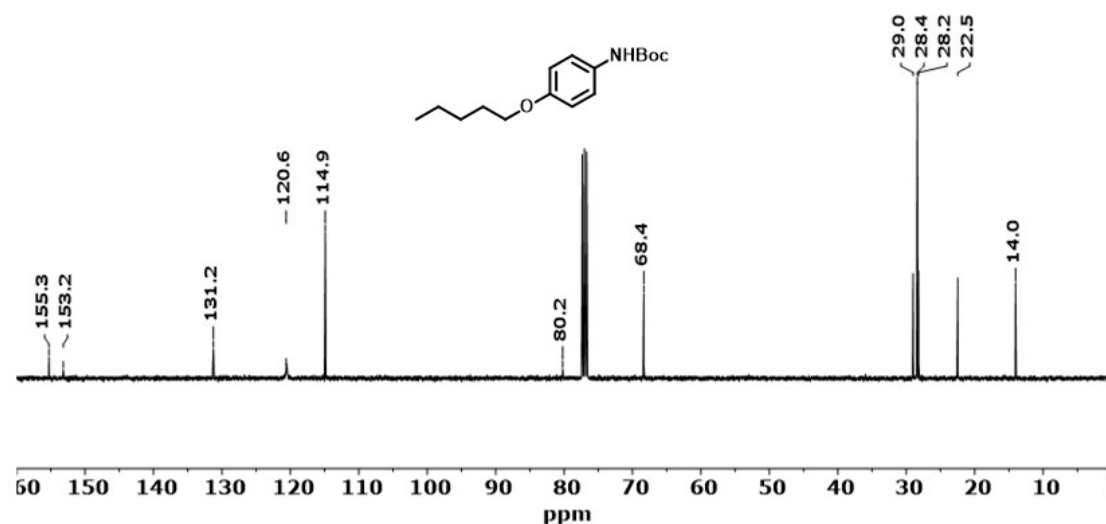


Figure S17. ^{13}C -NMR spectrum of **10** (Chloroform-*d*, 101 MHz): δ = 155.3 (-HN-**C**-O₂-), 153.2 (Ar-**C**-O-), 131.2 (Ar-**C**-NH**Boc**), 120.6 (Ar-**C**), 114.9 (Ar-**C**), 80.2 (-**C**-(**CH**₃)₃), 68.4 (-H₂**C**-O), 29.0 (-**CH**₂-), 28.4 (-**C**-(**CH**₃)₃), 28.2 (-**CH**₂-), 22.5 (-**CH**₂-**CH**₃), 14.0 (-**CH**₂-**CH**₃) ppm.

MS (*m/z*): (ESI, MeOH) Calculated for [**C**₁₆**H**₂₅**NO**₃**Na**]⁺: 302.1727; found 302.1736.

Synthesis of 4-(*n*-pentyloxy)aniline (**11**)

10 (545 mg, 1.95 mmol, 1.0 eq.) was dissolved in 6 mL of a mixture of DCM/TFA (1:1) and stirred under Argon at rt overnight. Thereafter, DCM was added (2× 50 mL) and evaporated to remove the TFA. After drying, compound **11** was used in the next step without further purification.

Yield: 600 mg (3.35 mmol, quant.).

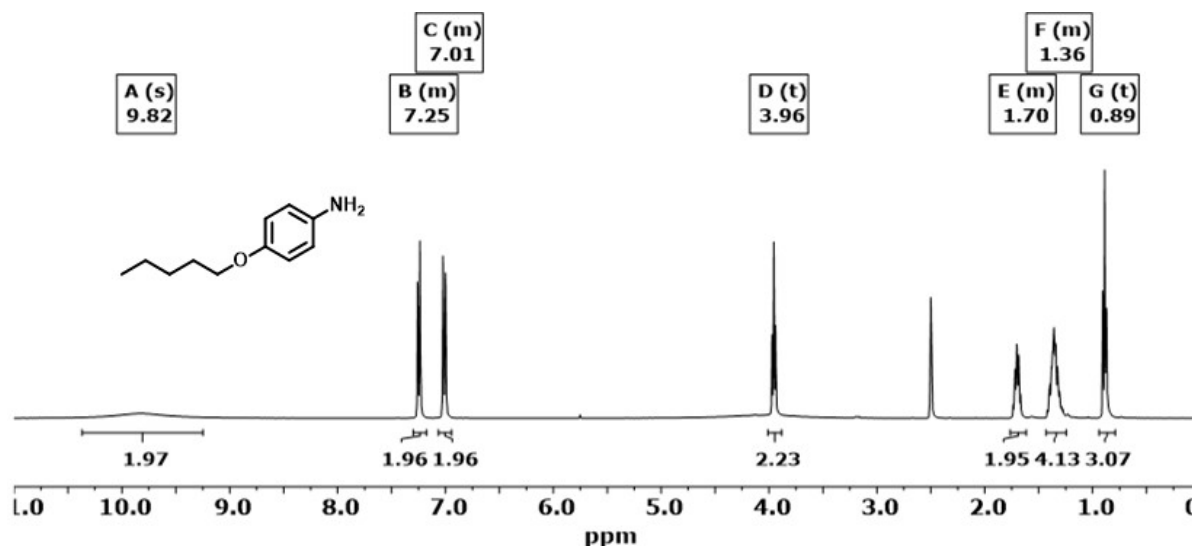


Figure S18. ¹H-NMR spectrum of **11** (DMSO-*d*₆, 400 MHz): δ = 9.82 (s, 2H, -NH₂), 7.30-7.14 (m, 2H, Ar-H), 7.09-6.92 (m, 2H, Ar-H), 3.96 (t, J = 6.5 Hz, 2H, O-CH₂-), 1.86-1.56 (m, 2H, -CH₂-), 1.48-1.28 (m, 4H, -(CH₂)₂-), 0.89 (t, J = 7.0 Hz, 3H, -CH₂-CH₃) ppm.

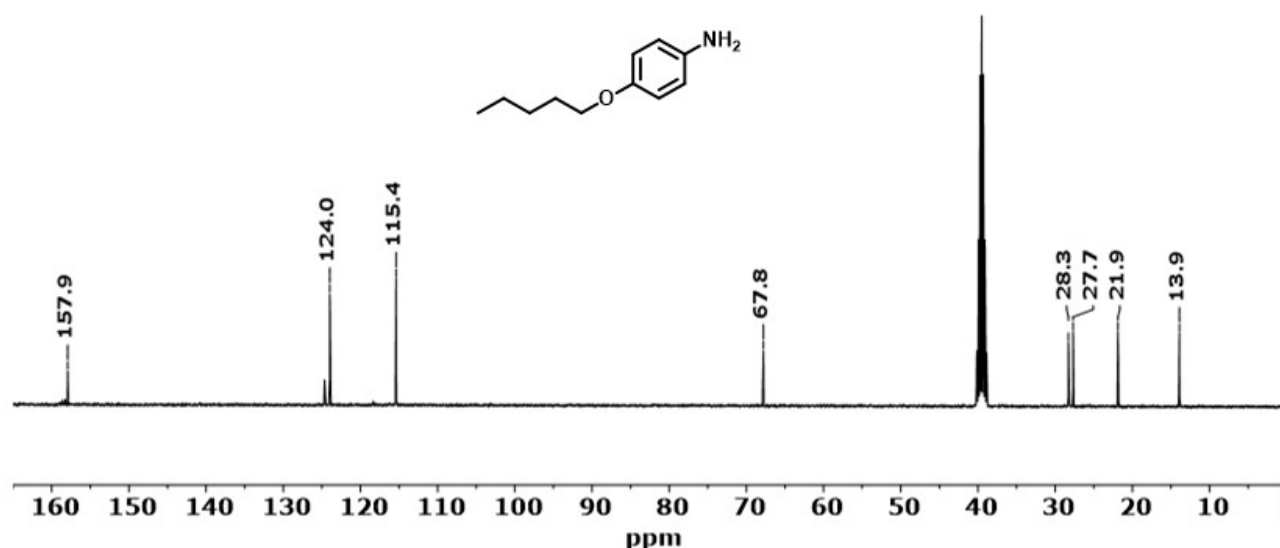


Figure S19. ¹³C-NMR spectrum of **11** (DMSO-*d*₆, 101 MHz): δ = 157.9 (Ar-C-O-), 124.0 (Ar-C), 115.4 (Ar-C), 67.8 (-H₂C-O), 28.3 (-CH₂-), 27.7 (-CH₂-), 21.9 (-CH₂-CH₃), 13.9 (-CH₂-CH₃) ppm.

MS (*m/z*): (ESI, MeOH) Calculated for [C₁₁H₁₇NOH]⁺: 180.1383; found 180.1400.

Synthetic Procedure for Compounds 5-8

General Procedure I: Synthesis of alkoxy 3-(2-phenylhydrazono)pentane-2,4-diones **5-8**

A solution of the substituted aniline (1.0 eq.) in AcOH (1.5 mL/mmol) and HCl (12 M, 0.23 mL/mmol) was cooled to 0 °C and NaNO₂ (1.2 eq.) in a small amount of H₂O was added dropwise. This mixture was stirred for 45 min at 0 °C. Afterwards the diazonium salt was added to a suspension of pentane-2,4-dione (1.3 eq.) and NaOAc (3.0 eq.) in a mixture of EtOH (1.0 mL/mmol) and H₂O (0.60 mL/mmol) and stirred overnight. The precipitate was filtered and washed several times with H₂O to yield the desired compound.

3-(2-(4-methoxyphenyl)hydrazineylidene)pentane-2,4-dione (5): Yield: 182 mg (0.777 mmol, 96%).

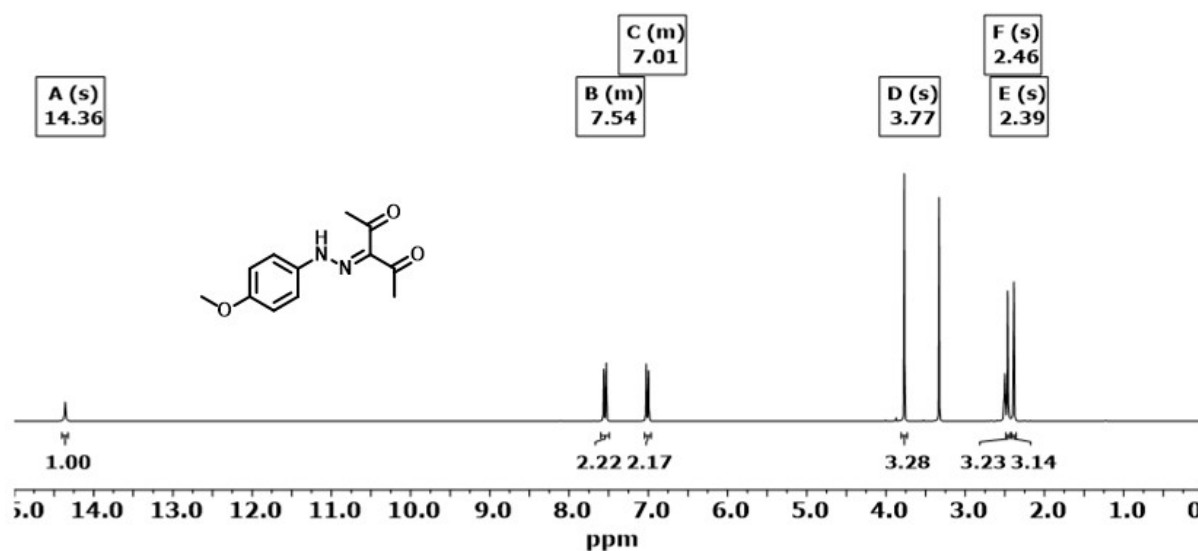


Figure S20. ¹H-NMR spectrum of **5** (DMSO-d₆, 300 MHz): δ = 14.36 (s, 1H, N-H), 7.61-7.48 (m, 2H, Ar-H), 7.08-6.96 (m, 2H, Ar-H), 3.77 (s, 3H, O-CH₃), 2.46 (s, 3H, -CH₃), 2.39 (s, 3H, -CH₃) ppm.

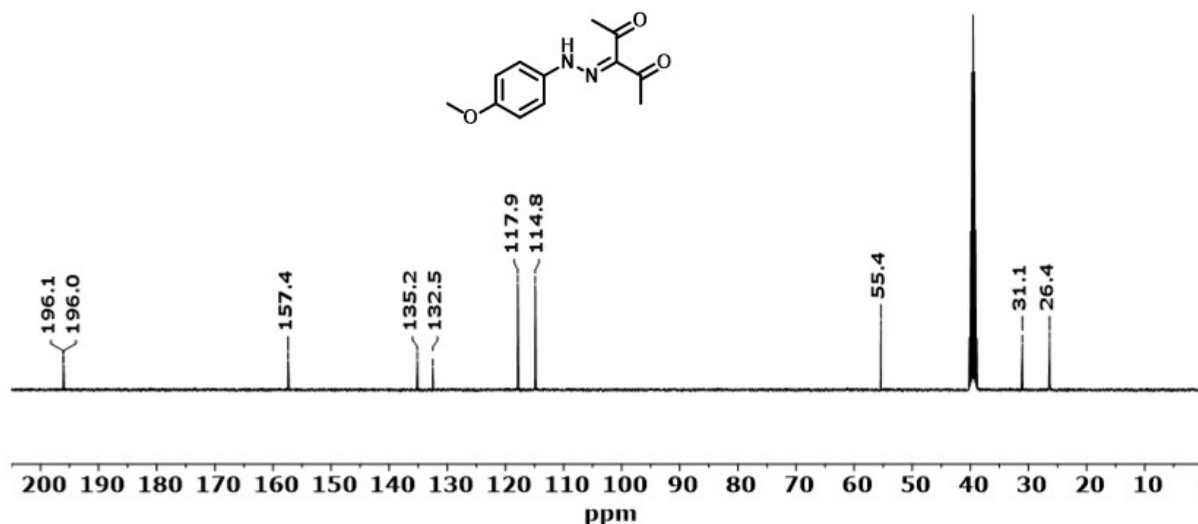


Figure S21. ^{13}C -NMR spectrum of **5** (DMSO- d_6 , 101 MHz): δ = 196.1, 196.0 (H₃C-(C=O)-), 157.4 (Ar-C-O-), 135.2 (C=N-), 132.5 (Ar=(C-NH)-Ar), 117.9 (Ar-C), 114.8 (Ar-C), 55.4 (H₃C-O), 31.1 (CH₃-), 26.4 (CH₃-) ppm.

MS (m/z): (ESI, MeOH) Calculated for [C₁₂H₁₄N₂O₃Na]⁺: 257.0902; found 257.0893.

3-(2-(4-(pentyloxy)phenyl)hydrazineylidene)pentane-2,4-dione (6): Yield: 507 mg (1.75 mmol, 81%).

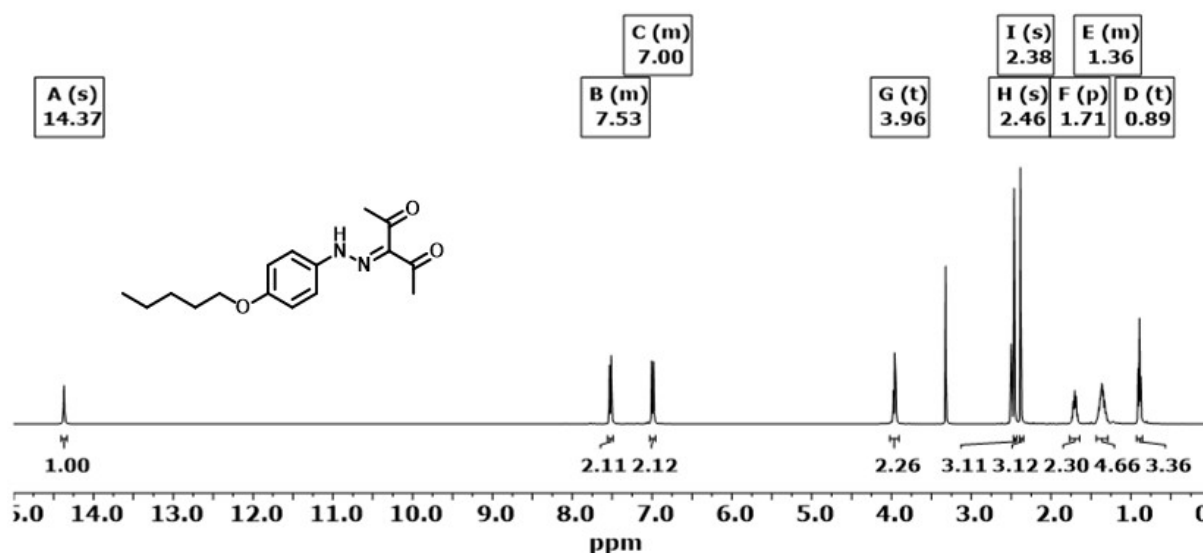


Figure S22. ^1H -NMR spectrum of **6** (DMSO- d_6 , 400 MHz): δ = 14.37 (s, 1H, N-H), 7.56-7.47 (m, 2H, Ar-H), 7.07-6.95 (m, 2H, Ar-H), 3.96 (t, J = 6.4 Hz, 2H, O-CH₂-), 2.46 (s, 3H, -CH₃), 2.38 (s, 3H, CH₃), 1.71 (p, J = 6.6 Hz, 2H, --CH₂-), 1.44 1.23 (m, 4H, (CH₂)₂-CH₃), 0.89 (t, J = 6.9 Hz, 3H, -CH₂ CH₃) ppm.

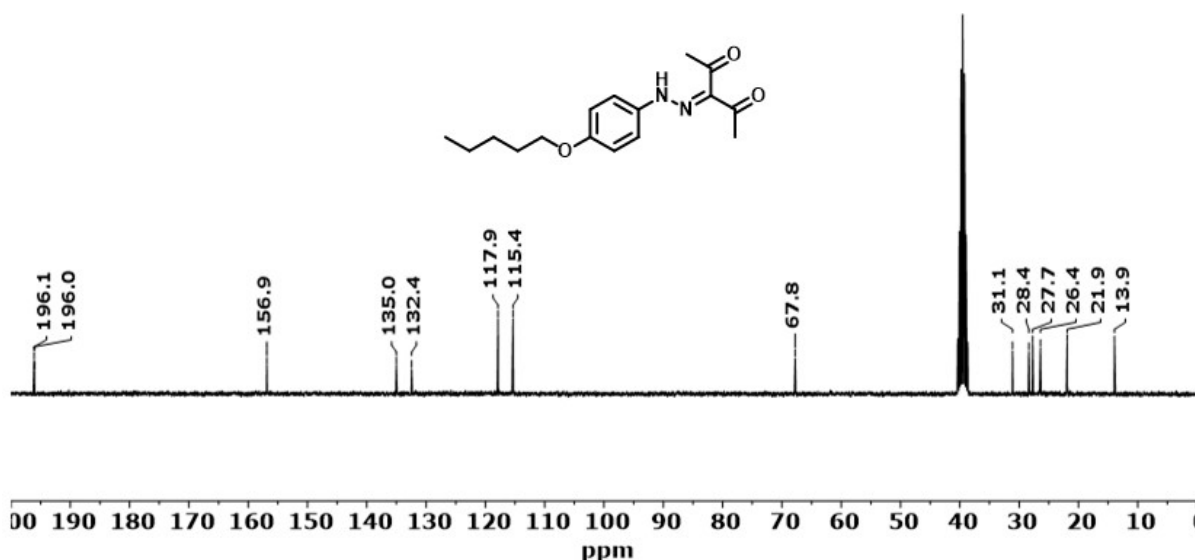


Figure S23. ^{13}C -NMR spectrum of **6** (DMSO- d_6 , 75 MHz): δ = 196.1, 196.0 (H₃C-(C=O)-), 156.9 (Ar-C-O-), 135.0 (C=N-), 132.4 (Ar=(C-NH)-Ar), 117.9 (Ar-C), 115.4 (Ar-C), 67.8 (-H₂C-O), 31.1 (-CH₂), 28.4 (-CH₂), 27.7 (CH₃-), 26.4 (CH₃-), 21.9 (-CH₂ CH₃), 13.9 (-CH₂-CH₃) ppm.

MS (m/z): (ESI, MeOH) Calculated for [C₁₆H₂₂N₂O₃Na]⁺: 313.1528; found 313.1518.

3-(2-(4-(n-hexyloxy)phenyl)hydrazineylidene)pentane-2,4-dione (7): Yield: 151 mg (0.496 mmol, 96%).

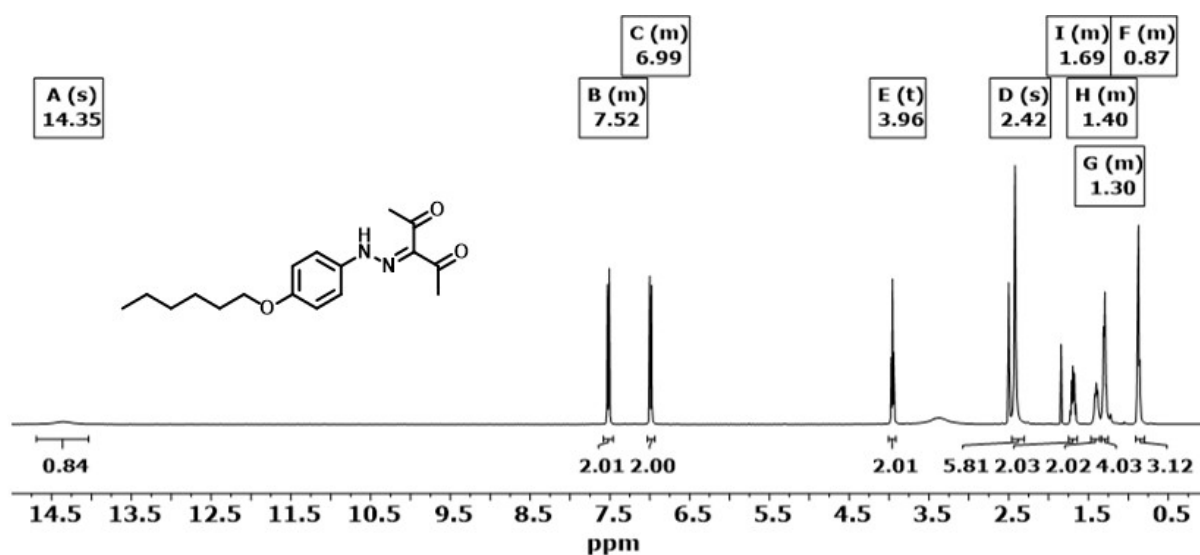


Figure S24. ^1H -NMR spectrum of **7** (DMSO- d_6 , 400 MHz): δ = 14.35 (s, 1H, N-H), 7.57-7.47 (m, 2H, Ar-H), 7.04-6.94 (m, 2H, Ar-H), 3.96 (t, J = 6.5 Hz, 2H, O-CH₂-), 2.42 (s, 6H, -CH₃), 1.76-1.63 (m, 2H, -CH₂-), 1.47-1.35 (m, 2H, -CH₂-), 1.35-1.25 (m, 4H, (CH₂)₂-CH₃), 0.92-0.80 (m, 3H, -CH₂ CH₃) ppm.

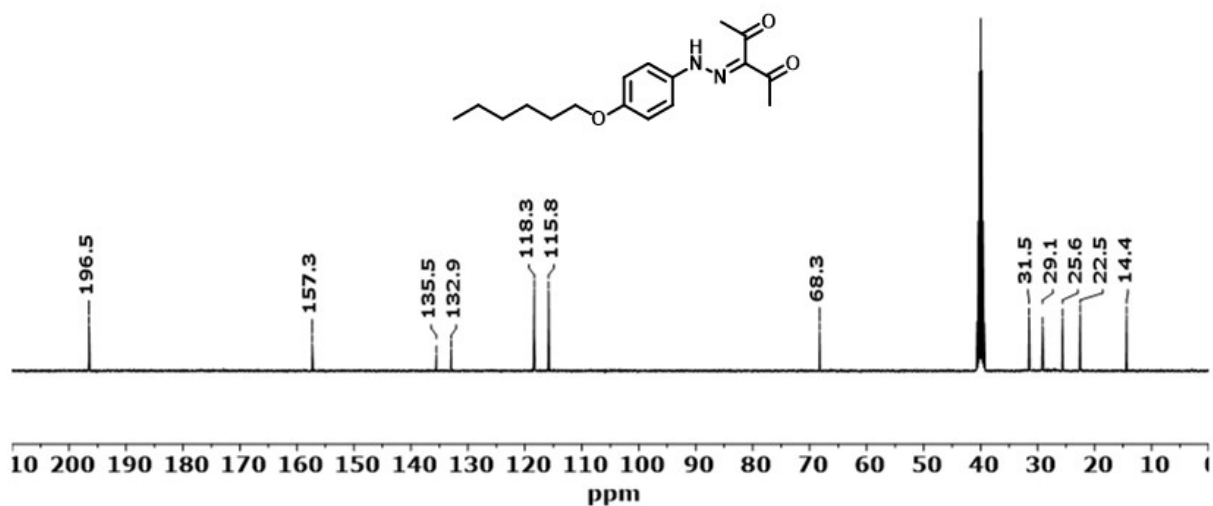


Figure S25. ^{13}C -NMR spectrum of **7** (DMSO- d_6 , 101 MHz): δ = 196.5 (H₃C-(C=O)-), 157.3 (Ar-C-O-), 135.6 (C=N-), 132.9 (Ar=(C-NH)-Ar), 118.3 (Ar-C), 115.8 (Ar-C), 68.3 (-H₂C-O), 31.5 (-CH₂), 29.1 (-CH₂), 25.7 (-CH₂-), 22.5 (-CH₂ CH₃), 14.4 (-CH₂-CH₃) ppm.

MS (m/z): (ESI, MeOH) Calculated for [C₁₇H₂₄N₂O₃Na]⁺: 327.1685; found 327.1684.

3-(2-(4-(n-nonyloxy)phenyl)hydrazineylidene)pentane-2,4-dione (8): Yield: 600 mg (1.73 mmol, 82%).

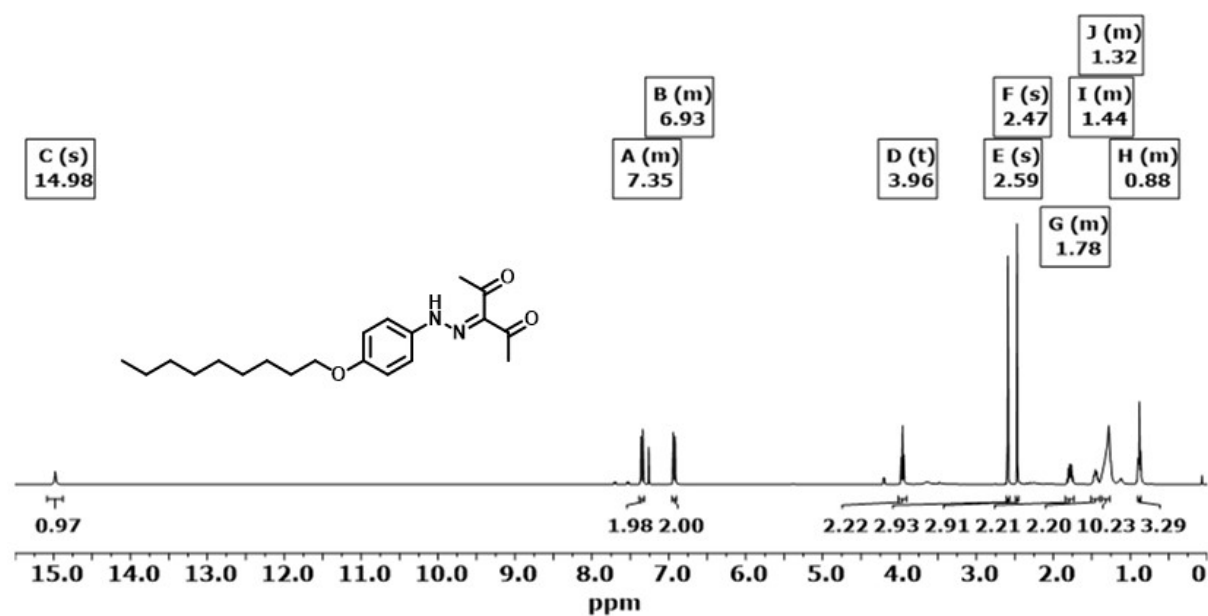


Figure S26. ^1H -NMR spectrum of **8** (Chloroform- d , 400 MHz): δ = 14.98 (s, 1H, N-H), 7.38-7.30 (m, 2H, Ar-H), 6.96-6.90 (m, 2H, Ar-H), 3.96 (t, J = 6.6 Hz, 2H, O-CH₂), 2.59 (s, 3H, -CH₃), 2.47 (s, 3H, CH₃), 1.91-1.68 (m, 2H, -CH₂-), 1.51-1.40 (m, 2H, -CH₂), 1.32-1.15 (m, 10H, (CH₂)₂-CH₃), 0.92-0.75 (m, 3H, -CH₂ CH₃) ppm.

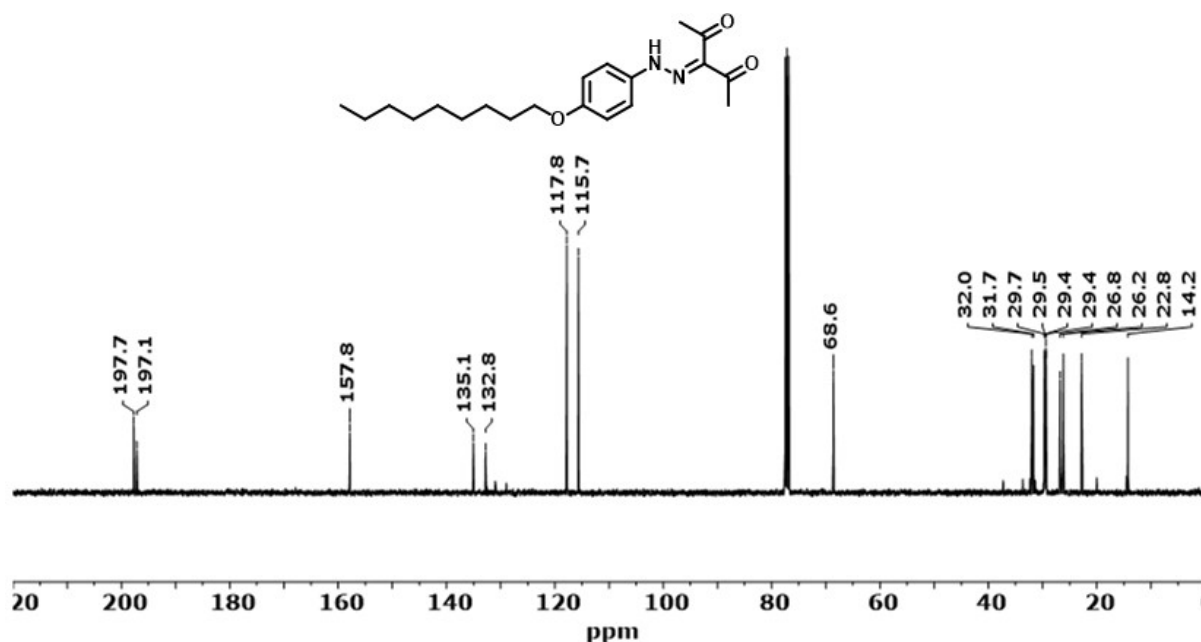


Figure S27. ¹³C-NMR spectrum of **8** (Chloroform-d, 101 MHz): δ = 197.7, 197.1 (H₃C-(C=O)-), 157.8 (Ar-C-O-), 135.1 (C=N-), 132.8 (Ar=(C-NH)-Ar), 117.8 (Ar-C), 115.7 (Ar-C), 68.6 (-H₂C-O), 32.0 (-CH₂), 31.7 (-CH₂), 29.7 (-CH₂-), 29.5 (-CH₂-), 29.4 (-CH₂-), 29.4 (-CH₂-), 26.8 (-CH₃), 26.2 (-CH₃), 22.8 (CH₂CH₃), 14.2 (-CH₂-CH₃) ppm.

MS (m/z): (ESI, MeOH) Calculated for [C₂₀H₃₀N₂O₃Na]⁺: 369.2149; found 369.2140.

Synthesis of Alkoxy-Substituted Arylazoisoxazoles (AIZs) 1-4

General Procedure II: To a suspension of **5-8** (1.0 eq.) in EtOH (10 mL/mmol) were added Na₂CO₃ (1.5 eq.) and hydroxylamine hydrochloride (1.5 eq.) and this mixture was stirred at 80 °C for 18 h. The solvent was removed under reduced pressure and the crude product was purified by column chromatography (silica, CH/EtOAc 20:1). After recrystallisation in EtOH the target molecule was washed with ice-cold EtOH (3×) and lyophilized to obtain a yellow solid in the yields listed below.

(E)-4-((4-methoxyphenyl)diazenyl)-3,5-dimethylisoxazole (1): Yield: 142 mg (0.614 mmol, 79%).

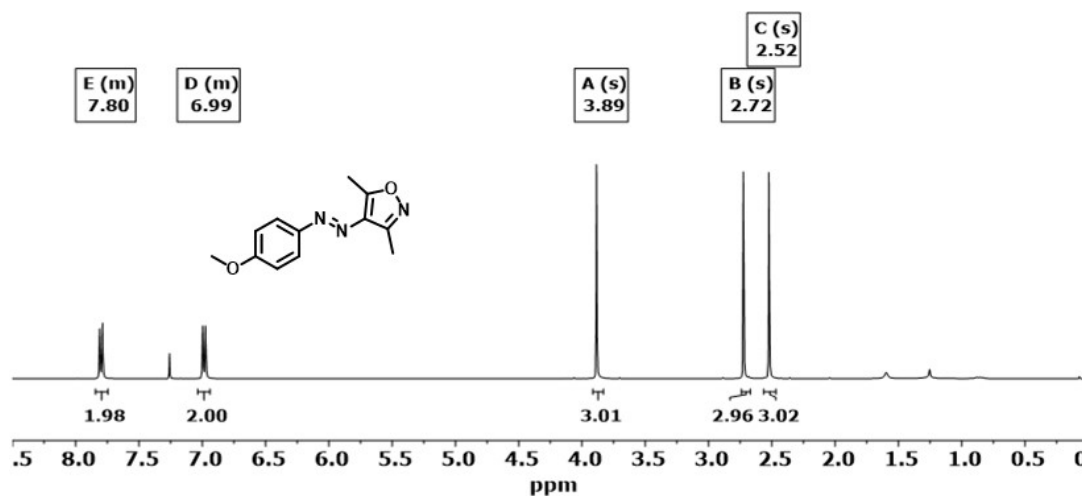


Figure S28. ^1H -NMR spectrum of **1** (Chloroform- d , 400 MHz): δ = 7.90-7.60 (m, 2H, Ar-H), 7.04-6.76 (m, 2H, Ar-H), 3.89 (s, 3H, O-CH₃), 2.72 (s, 3H, -CH₃), 2.52 (s, 3H, -CH₃) ppm.

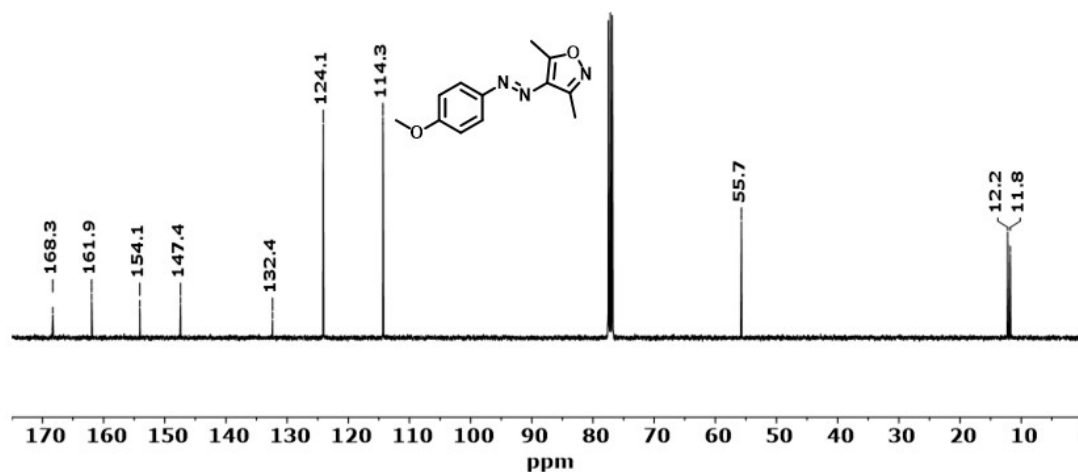


Figure S29. ^{13}C -NMR spectrum of **1** (Chloroform- d , 101 MHz): δ = 168.3 (H₃C-(C=O)=), 161.9 (Ar-C-OCH₃), 154.1 (H₃C (C=N)-), 147.4 (Ar-C-N=N-), 132.4 (Ar-C-N=N-C-), 124.1 (Ar-C), 114.3 (Ar-C), 55.7 (H₃C-O-), 12.2 (CH₃-), 11.8 (CH₃-) ppm.

MS (m/z): (ESI, MeOH) Calculated for [C₁₂H₁₃N₃O₂Na]⁺: 254.0900; found 254.0900.

CHN Analysis: Calculated C, 62.33; H, 5.67; N, 18.17; found C, 62.30; H, 5.76; N, 18.14.

(E)-3,5-dimethyl-4-((4-(n-pentyloxy)phenyl)diazenyl)isoxazole (2): Yield: 307 mg (1.07 mmol, 92%).

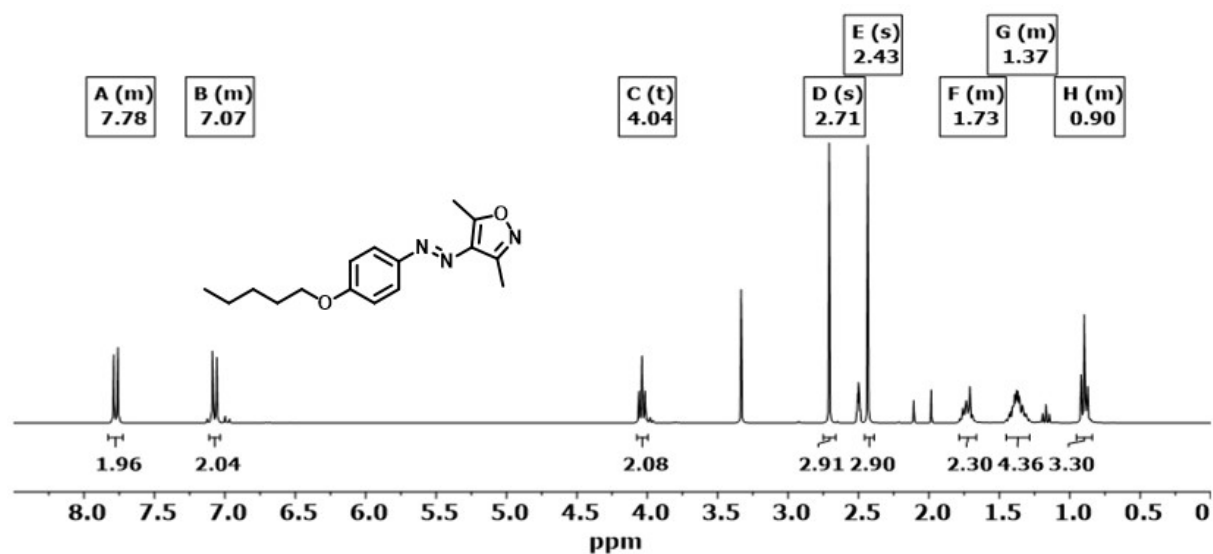


Figure S30. ^1H -NMR spectrum of **2** (DMSO- d_6 , 300 MHz): δ = 7.87-7.71 (m, 2H, Ar-H), 7.16-7.03 (m, 2H, Ar-H), 4.04 (t, J = 6.5 Hz, 2H, O-CH $_2$ -), 2.71 (s, 3H, -CH $_3$), 2.43 (s, 3H, CH $_3$), 1.84-1.66 (m, 2H, -CH $_2$ -), 1.47 1.28 (m, 4H, (CH $_2$) $_2$ -CH $_3$), 0.90 (m, 3H, -CH $_2$ CH $_3$) ppm.

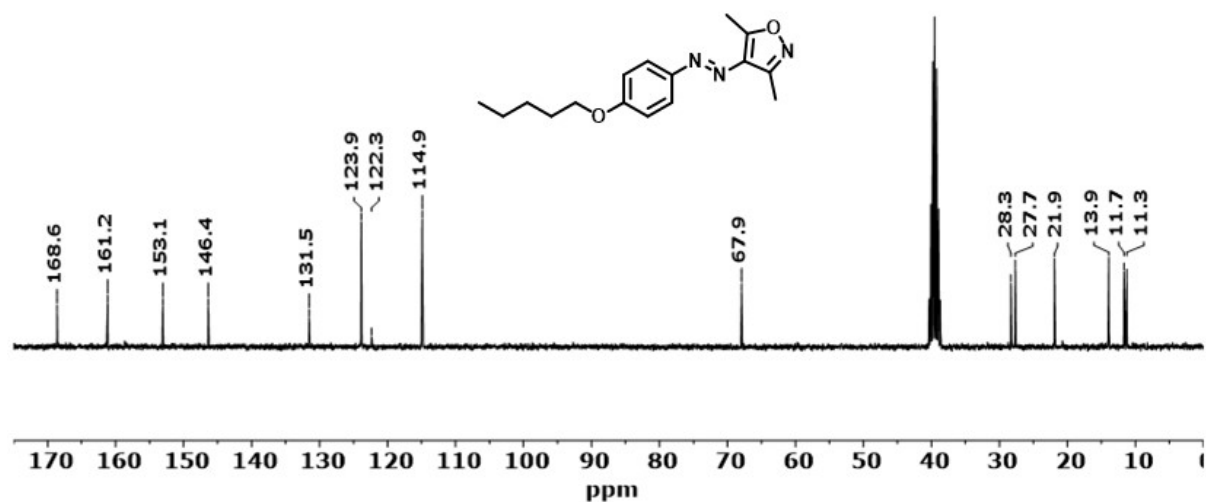


Figure S31. ^{13}C -NMR spectrum of **2** (DMSO- d_6 , 75 MHz): δ = 168.6 (H $_3$ C-(C=O)=), 161.2 (Ar-C-O-), 153.1 (H $_3$ C (C=N)-), 146.4 (Ar-C-N=N-), 131.5 (Ar-C-N=N-C-), 123.9 (Ar-C), 114.9 (Ar-C), 67.9 (H $_2$ C-O), 28.3 (-CH $_2$), 27.7 (-CH $_2$), 21.9 (-CH $_2$ CH $_3$), 13.9 (-CH $_2$ -CH $_3$), 11.7 (CH $_3$ -), 11.3 (CH $_3$) ppm.

MS (m/z): (ESI, MeOH) Calculated for $[\text{C}_{16}\text{H}_{21}\text{N}_3\text{O}_2\text{Na}]^+$: 310.1526; found 310.1533.

CHN Analysis: Calculated C, 66.88; H, 7.37; N, 14.62; found C, 66.65; H, 7.56; N, 14.57.

(E)-4-((4-(n-hexyloxy)phenyl)diazenyl)-3,5-dimethylisoxazole (3): Yield: 130 mg (0.431 mmol, 87%).

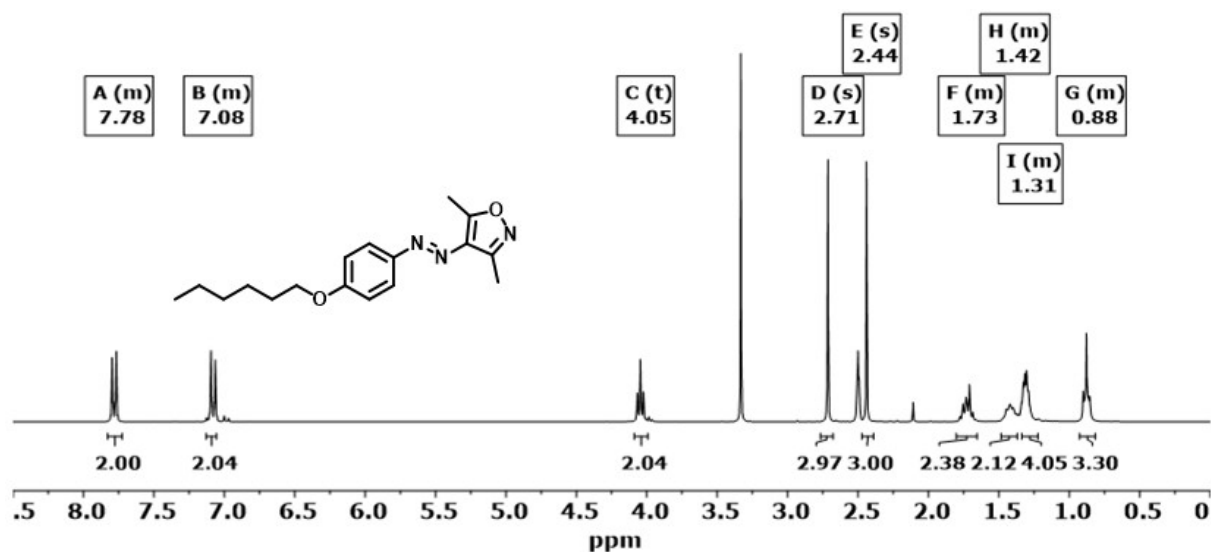


Figure S32. ^1H -NMR spectrum of **3** (DMSO- d_6 , 300 MHz): δ = 7.82-7.75 (m, 2H, Ar-H), 7.12-7.05 (m, 2H, Ar-H), 4.05 (t, J = 6.5 Hz, 2H, O-CH $_2$ -), 2.71 (s, 3H, -CH $_3$), 2.44 (s, 3H, CH $_3$), 1.84-1.64 (m, 2H, -CH $_2$ -), 1.48-1.38 (m, 2H, -CH $_2$ -) 1.35 1.26 (m, 4H, (CH $_2$) $_2$ -CH $_3$), 0.91-0.84 (m, 3H, -CH $_2$ CH $_3$) ppm.

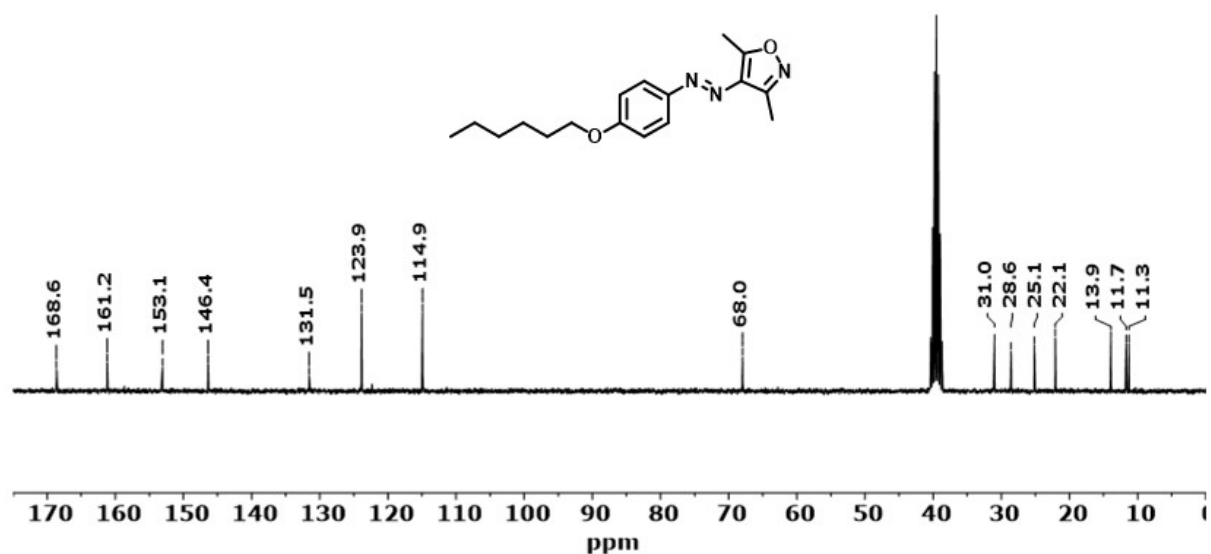


Figure S33. ^{13}C -NMR spectrum of **3** (DMSO- d_6 , 75 MHz): δ = 168.6 (H $_3$ C-(C=O)=), 161.2 (Ar-C-O-), 153.1 (H $_3$ C (C=N)-), 146.4 (Ar-C-N=N-), 131.5 (Ar-C-N=N-C-), 123.9 (Ar-C), 114.9 (Ar-C), 68.0 (H $_2$ C-O), 31.0 (CH $_2$ -), 28.6 (-CH $_2$), 25.2 (-CH $_2$), 22.1 (-CH $_2$ CH $_3$), 13.9 (-CH $_2$ -CH $_3$), 11.7 (CH $_3$ -), 11.3 (CH $_3$) ppm.

MS (m/z): (ESI, MeOH) Calculated for $[\text{C}_{17}\text{H}_{23}\text{N}_3\text{O}_2\text{Na}]^+$: 324.1682; found 324.1676.

CHN Analysis: Calculated C, 67.75; H, 7.69; N, 13.92; found C, 67.93; H, 7.79; N, 13.67.

(E)-3,5-dimethyl-4-((4-(n-nonyloxy)phenyl)diazenyl)isoxazole (4): Yield: 346 mg (1.01 mmol, 88%).

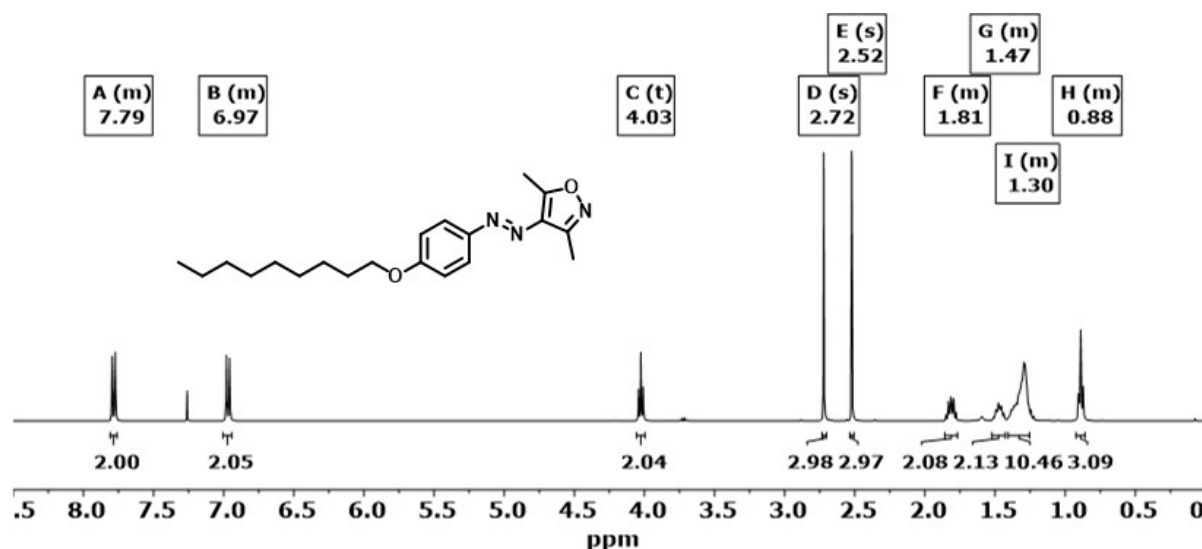


Figure S34. ^1H -NMR spectrum of **4** (Chloroform- d , 400 MHz): δ = 7.84-7.73 (m, 2H, Ar-H), 7.02-6.93 (m, 2H, Ar-H), 4.03 (t, J = 6.6 Hz, 2H, O-CH $_2$ -), 2.72 (s, 3H, -CH $_3$), 2.52 (s, 3H, CH $_3$), 1.88-1.74 (m, 2H, -CH $_2$ -), 1.54-1.43 (m, 2H, -CH $_2$ -) 1.39 1.21 (m, 10H, (CH $_2$) $_4$ -CH $_2$ -CH $_3$), 0.94-0.84 (m, 3H, -CH $_2$ CH $_3$) ppm.

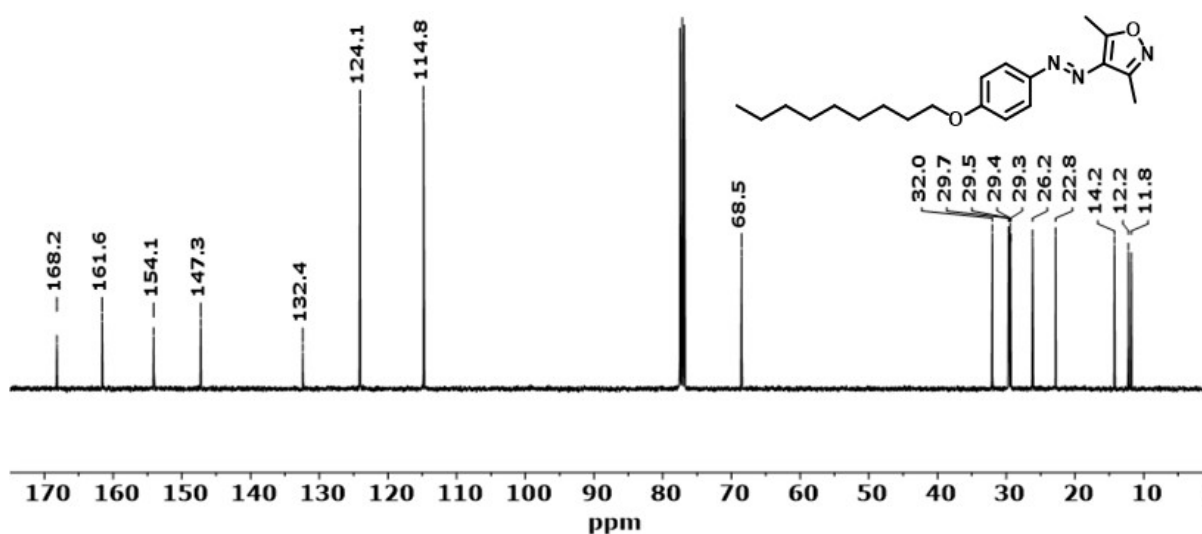


Figure S35. ^{13}C -NMR spectrum of **4** (Chloroform- d , 101 MHz): δ = 168.2 (H $_3$ C-(C=O)=), 161.6 (Ar-C-O-), 154.1 (H $_3$ C (C=N)-), 147.3 (Ar-C-N=N-), 132.4 (Ar-C-N=N-C-), 124.1 (Ar-C), 114.8 (Ar-C), 68.5 (H $_2$ C-O), 32.0 (CH $_2$ -), 29.7 (-CH $_2$ -), 29.5 (-CH $_2$ -), 29.4 (-CH $_2$ -), 29.3 (-CH $_2$ -), 26.2 (-CH $_2$ -), 22.8 (-CH $_2$ CH $_3$), 14.3 (-CH $_2$ -CH $_3$), 12.2 (CH $_3$ -), 11.8 (CH $_3$) ppm.

MS (m/z): (ESI, MeOH) Calculated for $[\text{C}_{20}\text{H}_{29}\text{N}_3\text{O}_2\text{Na}]^+$: 366.2152; found 366.2138.

CHN Analysis: Calculated C, 69.94; H, 8.51; N, 12.23; found C, 69.86; H, 8.28; N, 12.19.

Characterization Methods

UV/vis absorption spectra were recorded with a Jasco V750 double-beam spectrophotometer and processed with F. Menges' Spectragryph - optical spectroscopy software, v1.2.11. Irradiation of the samples in solution (acetonitrile) and in the solid state was carried out with light-emitting diodes at 365 nm (UV LED Gen2 Emitter, radiant flux 1.2 W, LED Engin Inc., San Jose, California, USA) and 520 nm (LSC-G HighPower-LED, radiant flux 87 lm, Cree Inc., Durham, North Carolina, USA). Monitoring of temperature during irradiation was done with an Etekcity Lasergrip 774 Infrared Thermometer. The NMR spectra for the characterization were recorded on an AV-300-spectrometer with 300.1 Hz (^1H) and 75.5 Hz (^{13}C) (Bruker, Billerica, Massachusetts, USA). For monitoring the photostationary states, a DD2-600-spectrometer with 600 Hz (^1H) and 151 Hz (^{13}C) was employed (Agilent Technologies, Santa Clara, California, USA). Chemical shifts (δ) are reported in parts per million with respect to tetramethylsilane, referenced to residual solvent (CD_2HCN , CD_2ClH or DMSO-d_5) signals, and coupling constants are denoted in hertz. Integrations are reported, with multiplicities denoted as: s = singlet, d = doublet, t = triplet, br = broad singlet, m = multiplet. MestReNova 12.0.4 (Mestrelab Research S.L., Santiago de Compostela, Spain) was used to analyze all NMR spectra. Mass spectra were recorded on a MicroTof ESI (Bruker Daltonics, Bremen, Germany) through Electrospray ionization (ESI) from methanol. Optical microscopy was performed with an Olympus CKX 41 microscope operated with an Olympus XC 10 camera, and their processing was done with the software Stream Essentials v1.9. Differential scanning calorimetry was conducted using a DSC Q2000 (TA instruments), with the samples hermetically sealed in aluminum TzeroTM pans. Tensile measurements were conducted on a Zwicki 1120 ZW2.5/TH1S tensile test machine. An Alpha 1-2 LD plus freeze dryer (Martin Christ GmbH, Osterode, Germany) was used for the lyophilization, in preparation all target compounds were suspended in ddH₂O and frozen under rotation in liquid nitrogen. Unless stated otherwise, ultrapure water with an electric resistance of > 18 M Ω (PurelabTM UHQ II water purification system, ELGA LabWater, High Wycombe, Buckinghamshire, UK) was used. Silica gel coated aluminium plates (model: 60 F254, Merck KGaA, Darmstadt, Germany) were employed for analytical thin layer chromatography. A Dual Wavelength UV Lamp (254 nm and 366 nm, CAMAG, Muttenz, Switzerland) or a basic permanganate solution was used to visualize the spots.

PSS and Thermal Half-Life Determinations

The PSS and the thermal half-life of compounds **1-4** were determined by using ^1H NMR Spectroscopy (DD2-600-spectrometer with 600 Hz). First, a stock solution (200 μM) in CD_3CN of each molecule was prepared. From this solution approx. 0.7 mL was taken and ^1H -NMR spectra of the thermal distribution of isomers were recorded. To avoid signal overlap in the analysis the chemical shift of the first methyl off the phenol moiety was selected, showing distinct and well-defined signals for both forms in all cases. To determine the PSS₃₆₅, the aforementioned stock solution was irradiated for 3 min with 365 nm to convert the thermally predominant *E*-isomer into the metastable *Z*-isomer, followed by immediate recording of their ^1H -NMR spectra. For the thermal half-life the NMR tubes with the *Z*-isomers were kept in the dark and ^1H -NMR spectra were taken after 4 and 7 days to analyze the *Z*-lifetime. Alternatively, by illumination with green light (520 nm, 2 min) the thermally stable *E*-isomers were recovered through the PSS₅₂₀ and their ^1H -NMR spectra were recorded. By analyzing the relative integrations of the *Z*- and *E*-isomer ^1H NMR signals the distribution of isomers at the PSSs could be determined, as well as the thermal reversion (and thus thermal half-life) of the *Z*-form.

Adhesion Experiments

Glass microscope slides (76 mm x 26 mm) from Servoprax GmbH, Wesel, Germany, were cut into 1.4 x 2.6 cm slides and washed with water and acetone. A scratch 1.0 cm into the slide marked the 1.4 cm² area on which 2.1 mg of AIZ was weighed out. Following a UV-induced solid-to-liquid phase transition, the liquid phase was pressed to a second slide and clamped with a household clothespin before facile green light-induced liquid-to-solid phase transitioning of the AIZ. For maximum weight determinations weights were hung incrementally from custom-made slide holders (with an inset depth shorter than the thickness of the glass slides, see Figure S7) until reaching the breaking point.

X-Ray diffraction

Data sets for compounds **2**, **3** and **4** were collected with a Bruker D8 Venture CMOS diffractometer. For compound **1** data sets were collected with a Bruker APEX II CCD diffractometer. Programs used: data collection: APEX3 V2016.1-0^[S4] (Bruker AXS Inc., **2016**); cell refinement: SAINT V8.37A (Bruker AXS Inc., **2015**); data reduction: SAINT V8.37A (Bruker AXS Inc., **2015**); absorption correction, SADABS V2014/7 (Bruker AXS

Inc., **2014**); structure solution *SHELXT-2015*^[S5] (Sheldrick, G. M. *Acta Cryst.*, **2015**, *A71*, 3-8); structure refinement *SHELXL-2015*^[S6] (Sheldrick, G. M. *Acta Cryst.*, **2015**, *C71* (1), 3-8) and graphics, *XP*^[S7] (Version 5.1, Bruker AXS Inc., Madison, Wisconsin, USA, **1998**). *R*-values are given for observed reflections, and *wR*² values are given for all reflections.

Exceptions and special features: For compound **6** the isoxazole unit is disordered over two positions. Several restraints (SADI, SAME, ISOR and SIMU) were used in order to improve refinement stability.

X-ray crystal structure analysis of 1

A yellow prism-like specimen of C₁₂H₁₃N₃O₂, approximate dimensions 0.040 mm x 0.280 mm x 0.360 mm, was used for the X-ray crystallographic analysis. The X-ray intensity data were measured. A total of 1293 frames were collected. The total exposure time was 20.84 hours. The frames were integrated with the Bruker SAINT software package using a wide-frame algorithm. The integration of the data using a triclinic unit cell yielded a total of 14418 reflections to a maximum θ angle of 66.72° (0.84 Å resolution), of which 3885 were independent (average redundancy 3.711, completeness = 95.5%, *R*_{int} = 5.02%, *R*_{sig} = 4.61%) and 2798 (72.02%) were greater than 2 σ (*F*²). The final cell constants of *a* = 9.5348(4) Å, *b* = 9.6604(3) Å, *c* = 13.3499(5) Å, α = 74.304(2)°, β = 89.794(2)°, γ = 76.578(2)°, volume = 1149.17(8) Å³, are based upon the refinement of the XYZ-centroids of 4590 reflections above 20 σ (*I*) with 6.891° < 2 θ < 133.2°. Data were corrected for absorption effects using the multi-scan method (SADABS). The ratio of minimum to maximum apparent transmission was 0.817. The calculated minimum and maximum transmission coefficients (based on crystal size) are 0.7690 and 0.9700. The structure was solved and refined using the Bruker SHELXTL Software Package, using the space group *P*-1, with *Z* = 4 for the formula unit, C₁₂H₁₃N₃O₂. The final anisotropic full-matrix least-squares refinement on *F*² with 312 variables converged at *R*1 = 4.69%, for the observed data and *wR*2 = 12.51% for all data. The goodness-of-fit was 1.040. The largest peak in the final difference electron density synthesis was 0.276 e⁻/Å³ and the largest hole was -0.276 e⁻/Å³ with an RMS deviation of 0.051 e⁻/Å³. On the basis of the final model, the calculated density was 1.337 g/cm³ and *F*(000), 488 e⁻. CCDC Nr.: 1960718.

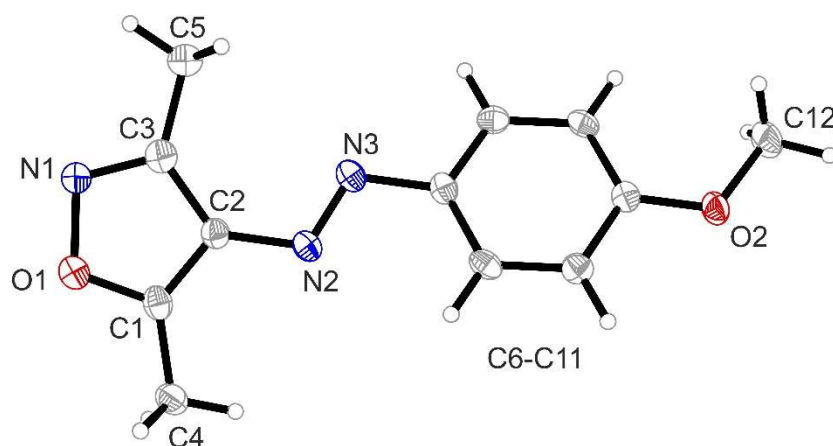


Figure S36. Crystal structure of compound 1. One of two molecules

(molecule “A”) found in the asymmetric unit is shown.

Thermal ellipsoids are shown at 50% probability.

X-ray crystal structure analysis of 2

A yellow prism-like specimen of $C_{16}H_{21}N_3O_2$, approximate dimensions 0.167 mm x 0.174 mm x 0.305 mm, was used for the X-ray crystallographic analysis. The X-ray intensity data were measured. A total of 688 frames were collected. The total exposure time was 7.64 hours. The frames were integrated with the Bruker SAINT software package using a narrow-frame algorithm. The integration of the data using a monoclinic unit cell yielded a total of 22682 reflections to a maximum θ angle of 25.36° (0.83 \AA resolution), of which 2824 were independent (average redundancy 8.032, completeness = 99.6%, $R_{\text{int}} = 7.84\%$, $R_{\text{sig}} = 4.01\%$) and 2293 (81.20%) were greater than $2\sigma(F^2)$. The final cell constants of $a = 5.3200(3) \text{ \AA}$, $b = 38.933(3) \text{ \AA}$, $c = 7.6411(6) \text{ \AA}$, $\beta = 102.459(2)^\circ$, volume = $1545.38(19) \text{ \AA}^3$, are based upon the refinement of the XYZ-centroids of 5118 reflections above $20 \sigma(I)$ with $5.559^\circ < 2\theta < 50.67^\circ$. Data were corrected for absorption effects using the multi-scan method (SADABS). The ratio of minimum to maximum apparent transmission was 0.851. The calculated minimum and maximum transmission coefficients (based on crystal size) are 0.9750 and 0.9860. The structure was solved and refined using the Bruker SHELXTL Software Package, using the space group $P2_1/c$, with $Z = 4$ for the formula unit, $C_{16}H_{21}N_3O_2$. The final anisotropic full-matrix least-squares refinement on F^2 with 193 variables converged at $R1 = 6.45\%$, for the observed data and $wR2 = 13.83\%$ for all data. The goodness-of-fit was 1.149. The largest peak in the final difference electron density synthesis was $0.211 \text{ e}/\text{\AA}^3$ and the largest hole was

-0.273 e⁻/Å³ with an RMS deviation of 0.051 e⁻/Å³. On the basis of the final model, the calculated density was 1.235 g/cm³ and F(000), 616 e⁻. CCDC Nr.: 1960719.

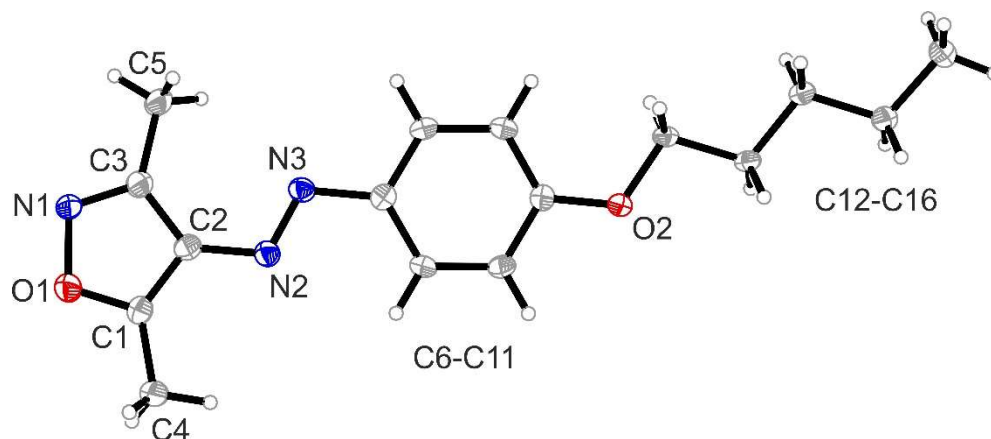


Figure S37. Crystal structure of compound 5.

Thermal ellipsoids are shown at 50% probability.

X-ray crystal structure analysis of 3

A yellow plate-like specimen of C₁₇H₂₃N₃O₂, approximate dimensions 0.040 mm x 0.136 mm x 0.144 mm, was used for the X-ray crystallographic analysis. The X-ray intensity data were measured. A total of 678 frames were collected. The total exposure time was 3.77 hours. The frames were integrated with the Bruker SAINT software package using a narrow-frame algorithm. The integration of the data using a triclinic unit cell yielded a total of 12578 reflections to a maximum θ angle of 25.37° (0.83 Å resolution), of which 3018 were independent (average redundancy 4.168, completeness = 99.5%, R_{int} = 2.92%, R_{sig} = 2.30%) and 2635 (87.31%) were greater than 2 $\sigma(F^2)$. The final cell constants of a = 6.3403(3) Å, b = 8.1035(4) Å, c = 17.1818(8) Å, α = 94.080(2)°, β = 91.396(2)°, γ = 110.323(2)°, volume = 824.59(7) Å³, are based upon the refinement of the XYZ-centroids of 4697 reflections above 20 $\sigma(I)$ with 5.380° < 2 θ < 50.67°. Data were corrected for absorption effects using the multi-scan method (SADABS). The ratio of minimum to maximum apparent transmission was 0.946. The calculated minimum and maximum transmission coefficients (based on crystal size) are 0.9880 and 0.9970. The structure was solved and refined using the Bruker SHELXTL Software Package, using the space group $P\bar{1}$, with Z = 2 for the formula unit, C₁₇H₂₃N₃O₂. The final anisotropic full-matrix least-squares refinement on F^2 with 238 variables converged at $R1$ = 4.34%, for the observed data and $wR2$ = 9.99% for all data. The goodness-of-fit was 1.037. The largest peak in the final difference electron density synthesis

was $0.354 \text{ e}^-/\text{\AA}^3$ and the largest hole was $-0.204 \text{ e}^-/\text{\AA}^3$ with an RMS deviation of $0.036 \text{ e}^-/\text{\AA}^3$. On the basis of the final model, the calculated density was 1.214 g/cm^3 and $F(000)$, 324 e^- . CCDC Nr.: 1960720.

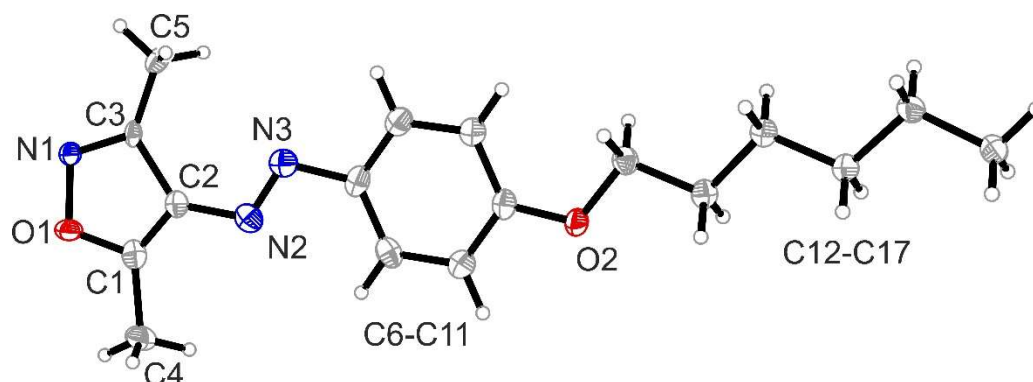


Figure S38. Crystal structure of compound 6.

Thermal ellipsoids are shown at 50% probability.

X-ray crystal structure analysis of 4

A yellow plate-like specimen of $\text{C}_{20}\text{H}_{29}\text{N}_3\text{O}_2$, approximate dimensions $0.041 \text{ mm} \times 0.185 \text{ mm} \times 0.188 \text{ mm}$, was used for the X-ray crystallographic analysis. The X-ray intensity data were measured. A total of 1532 frames were collected. The total exposure time was 22.38 hours. The frames were integrated with the Bruker SAINT software package using a wide-frame algorithm. The integration of the data using a monoclinic unit cell yielded a total of 22841 reflections to a maximum θ angle of 68.47° (0.83 \AA resolution), of which 3494 were independent (average redundancy 6.537, completeness = 99.3%, $R_{\text{int}} = 7.16\%$, $R_{\text{sig}} = 4.47\%$) and 2682 (76.76%) were greater than $2\sigma(F^2)$. The final cell constants of $a = 5.83910(10) \text{ \AA}$, $b = 41.5246(9) \text{ \AA}$, $c = 7.9955(2) \text{ \AA}$, $\beta = 98.3570(10)^\circ$, volume = $1918.05(7) \text{ \AA}^3$, are based upon the refinement of the XYZ-centroids of 7264 reflections above $20 \sigma(I)$ with $8.517^\circ < 2\theta < 136.7^\circ$. Data were corrected for absorption effects using the multi-scan method (SADABS). The ratio of minimum to maximum apparent transmission was 0.777. The calculated minimum and maximum transmission coefficients (based on crystal size) are 0.8930 and 0.9750. The structure was solved and refined using the Bruker SHELXTL Software Package, using the space group $P2_1/c$, with $Z = 4$ for the formula unit, $\text{C}_{20}\text{H}_{29}\text{N}_3\text{O}_2$. The final anisotropic full-matrix least-squares refinement on F^2 with 229 variables converged at $R1 = 4.65\%$, for the observed data and $wR2 = 12.13\%$ for all data. The goodness-of-fit was 1.064. The largest peak in the final difference electron density synthesis was $0.181 \text{ e}^-/\text{\AA}^3$ and the

largest hole was $-0.208 \text{ e}^-/\text{\AA}^3$ with an RMS deviation of $0.041 \text{ e}^-/\text{\AA}^3$. On the basis of the final model, the calculated density was 1.189 g/cm^3 and $F(000)$, 744 e^- . CCDC Nr.: 1960721.

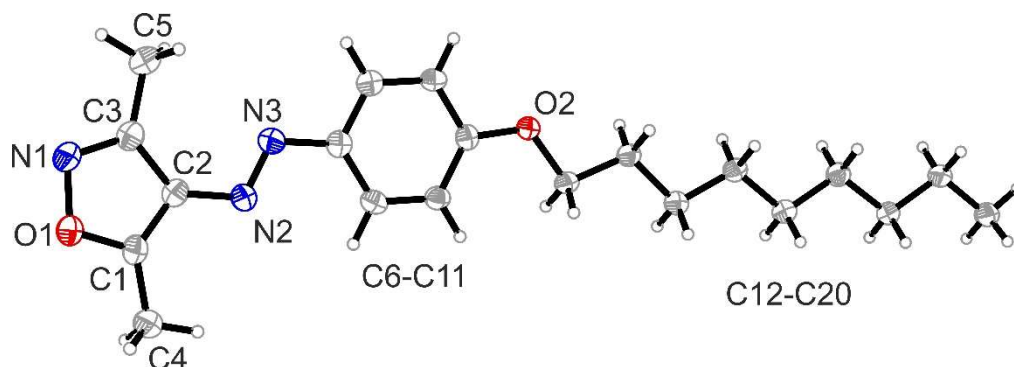


Figure S39. Crystal structure of compound 9.

Thermal ellipsoids are shown at 50% probability.

SUPPORTING REFERENCES

- [S1] Weston, C. E.; Richardson, R. D.; Haycock, P. R.; White, A. J. P.; Fuchter, M. J. Arylazopyrazoles: Azoheteroarene Photoswitches Offering Quantitative Isomerization and Long Thermal Half-Lives. *J. Am. Chem. Soc.* **2014**, *136*, 11878-11881.
- [S2] Kumar, P.; Srivastava, A.; Sah, C.; Devi, S.; Venkataramani, S. Arylazo-3,5-dimethylisoxazoles: Azoheteroarene Photoswitches Exhibiting High Z-Isomer Stability, Solid-State Photochromism, and Reversible Light-Induced Phase Transition. *Chem. Eur. J.* **2019**, *25*, 11924-11932.
- [S3] Forshaw, S.; Matthews, A. J.; Brown, T. J.; Diorazio, L. J.; Williams, L.; Wills, M. Asymmetric Transfer Hydrogenation of 1,3-Alkoxy/Aryloxy Propanones Using Tethered Arene/Ru(II)/TsDPEN Complexes. *Org. Letters* **2017**, *19*, 2789-2792.
- [S4] (a) *APEX3*; Bruker AXS Inc.: Madison, Wisconsin, USA, **2016**. (b) *SAINT*; Bruker AXS Inc.: Madison, Wisconsin, USA, **2015**. (c) *SADABS*; Bruker AXS Inc.: Madison, Wisconsin, USA, **2015**.
- [S5] Sheldrick, G. M. SHELXT – Integrated Space-Group and Crystal-Structure Determination, *Acta Cryst.*, **2015**, *A71*, 3-8.
- [S6] Sheldrick, G.M. Crystal Structure Refinement with SHELXL. *Acta Cryst.*, **2015**, *C71* (1), 3-8.
- [S7] *XP – Interactive molecular graphics*, Version 5.1; Bruker AXS Inc.: Madison, Wisconsin, USA, **1998**.